MODELING WATER FLUX IN FORWARD OSMOSIS: IMPLICATIONS FOR IMPROVED MEMBRANE DESIGN

by

Muna Al Mazrooei

A Thesis Presented to the Faculty of the
American University of Sharjah
College of Engineering
in Partial Fulfillment
of the Requirements
for the Degree of

Master of Science in
Chemical Engineering

Sharjah, United Arab Emirates

May 2013

Approval Signatures

We, the undersigned, approve the Master's Thesis of Muna Almazrooei.

Thesis Title: Modeling water flux in forward osmosis: Implications for improved membrane design

Signature	**Date of Signature**
_____	_____
Dr. Raafat Alnaizy Associate Professor Thesis Advisor	
_____	_____
Dr. Ahmed Aidan Lab Instructor Thesis Advisor	
_____	_____
Dr. Zarook Shareefdeen Associate Professor Thesis Committee Member	
_____	_____
Dr. Serter Atabay Associate Professor Thesis Committee Member	
_____	_____
Dr. Naif Abdelaziz Darwish Professor and Interim Department Head	
_____	_____
Dr. Hany El-Kadi Associate Dean of Engineering	
_____	_____
Dr. Hany El-Kadi Associate Dean of Engineering	
_____	_____
Dr. Khaled Assaleh Director of Graduate Studie	

Abstract

In efforts to make fresh water available to all people, researchers are dedicated to establish a water treatment method that will reduce the cost of production and impact on the environment. Forward osmosis desalination has been under the spotlight as a candidate of being a revolutionary water treatment method. Nevertheless, forward osmosis is faced with obstacles that hinder it from being commercially available. One of the main forward osmosis problems is low flux induced by concentration polarization and inadequate membrane design. To examine the problem, a commercially available forward osmosis membrane was tested using two different draw solutions. Using different feed solutions, experimental flux was determined and flux modeling was performed for the system in hand. The flux model selected was a good fit to experimental data for all draw solutions used; NaCl, magnesium sulfate and copper sulfate. The model was tested on our experimental data and other researchers' data. The flux model was found to be in line with experimental data for all systems at various operating conditions. It was found that dilutive internal concentration polarization (ICP) had a significant impact on flux. The overall driving force was reduced by dilutive ICP which caused a substantial reduction in the flux. It was determined that to reduce Dilutive ICP, solute resistance to diffusion (K) had to be minimized. Results also indicated that minimizing solute resistance to diffusion (K) achieved higher flux. It was also concluded that concentrative external concentration polarization (ECP) had a minor impact on flux. Varying feed mass transfer coefficient, a factor controlling concentrative ECP, had a small effect on flux. Magnesium sulfate and copper sulfate draw solutions were compared in terms of flux; it was found that coppers sulfate generates higher flux.

Search Terms: forward osmosis, concentration polarization, membrane, draw solution, modeling

Table of Contents

List of Figures

List of Tables

Nomenclature

A – Pure water permeability coefficient (m/s·atm)

A_m – effective membrane area (cm^2)

B – Salt permeability coefficient of the active layer (m/s)

D – Diffusion coefficient (m^2/s)

J_w – Flux ($L/m^2 \cdot h$)

k – Mass transfer coefficient (m/s)

K – Solute resistance to diffusion (s/m)

t – Thickness (μm)

ppm – parts per million (mg/l)

ΔV – change in volume (ml)

Δt – change in time (min)

$\pi_{D,b}$ – Osmotic pressure of bulk draw solution (atm)

$\pi_{D,i}$ – Osmotic pressure of draw solution inside the active layer within the porous support (atm)

$\pi_{D,m}$ – Osmotic pressure of draw solution at membrane surface (atm)

$\pi_{F,b}$ – Osmotic pressure of bulk feed solution (atm)

$\pi_{F,i}$ – Osmotic pressure of feed solution inside the active layer within the porous support (atm)

$\pi_{F,m}$ – Osmotic pressure of feed solution at membrane surface (atm)

τ – Tortuosity

ε – Porosity of the support layer

Chapter1: Introduction

1.1. Thesis Contribution

With the growth of interest toward FO processes as an alternative water desalination method, continuous improvements in the field are explored, especially in membrane development and draw solution development. In this research a commercially available forward osmosis membrane was tested. Based on flux modeling, parameters affecting forward osmosis membrane design and flux were studied. Various draw solutions (NaCl and $MgSO_4$ solutions) were used to investigate and optimize the effects of various operating conditions on the flux

1.2. Thesis Objective

Forward Osmosis studies have recently increased to assess the process limitations of the process. Most of the studies are to estimate and evaluate the effect of ICP and ECP. The thesis objectives are

- to model the flux;
- to study the effect of ECP and dilutive ICP on flux;
- to identify which phenomena controls flux;
- to study the effectiveness of different draw solutions based on osmotic pressure;
- to compare the experimental flux vs. the theoretical flux;
- to carry out a sensitivity analysis to evaluate effects of membrane structural characteristics;
- to investigate the effect of water permeability coefficient, solute resistance to diffusion, and mass transfer coefficients of feed and draw solutions; and
- to propose changes in membrane design and structural characteristics for performance improvements.

1.3. Thesis Organization

In the first chapter, a brief description on alternative water desalination methods is given to display current methods of water desalination. It is followed by an explanation about the forward osmosis process with its applications. Modeling equations are also displayed then draw solution and membrane selections are explained. Chapter 2 covers methodology to obtain the required data and the calculation procedure. Chapter 3 covers the results and discussion ending with the conclusion in Chapter 4.

1.4 .Background and Literature Review

Water is the base of all living things. On it rests the foundation of human health, wellbeing and most importantly the environment. On the other hand 4 out of 10 people [1] do not have access to fresh water, and some 2.8 million people die of water related diseases according to [2]. In addition, the continuous growth of the human population that has reached 80 million per year [3] adds stress on the currently vulnerable fresh water supply. Water consumption worldwide is distributed for domestic, irrigation and industry. Northern African and West Asian countries are considered to be water scarce and the situation is expected to worsen in the future. Figure 1 below shows the areas expected with water scarcity by the year 2030.

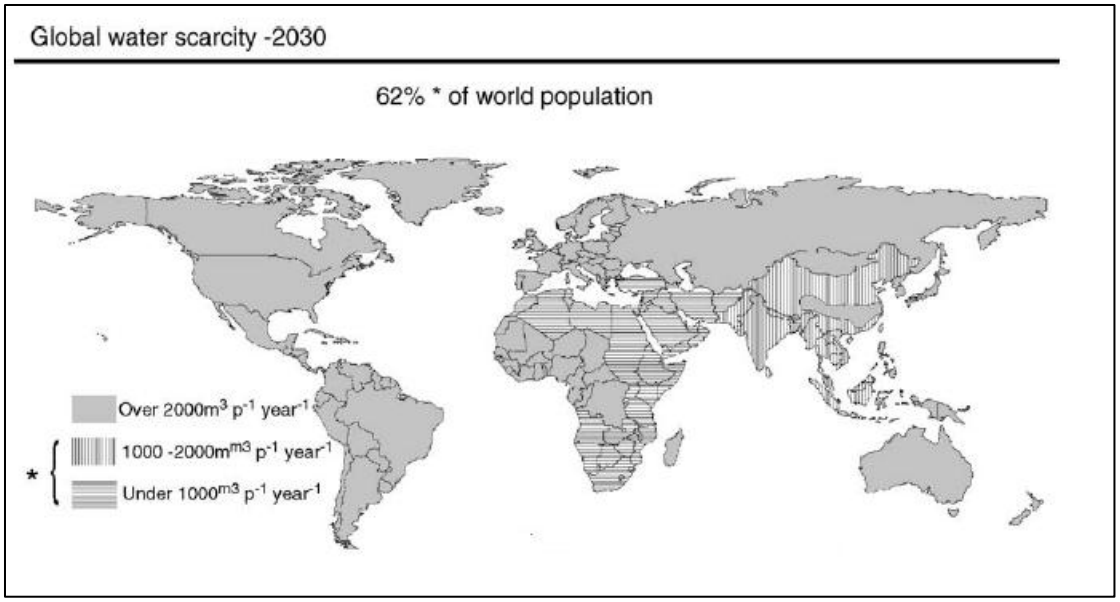

Figure 1: Water scarcity based on Falkenmark indicator [2]

Great effort has been dedicated to ensure the sustainability of fresh drinking water, such as the United Nations (UN) initiative to reduce the population with no access to drinking water to half by introducing the International Decade of Action 'Water for Life' 2005-2015. As known, the water distribution is 97.5% salt water and the remaining 2.5% is fresh water. Many areas depend on ground water and rivers as a source of fresh water, but the rate of consumption exceeds the rate required to replenish the quantity of the available fresh water putting the system under stress. Areas where fresh water is not available resort to water desalination as a source of fresh water. The efforts of researchers are dedicated to either improve existing water production systems or propose alternative methods that offer competitive advantages over current systems.

1.5. Conventional Desalination Methods

Water desalination processes are usually designed to split the feed stream into two streams; concentrated brine and a product with low concentration of dissolved solids. A form of energy is required to achieve the process, among all of the water desalination processes known the most common are multi-stage flash distillation and reverse osmosis.

Figure 2 and 3 shows the distribution of water production according to technology. The two main technologies used in industry are described below.

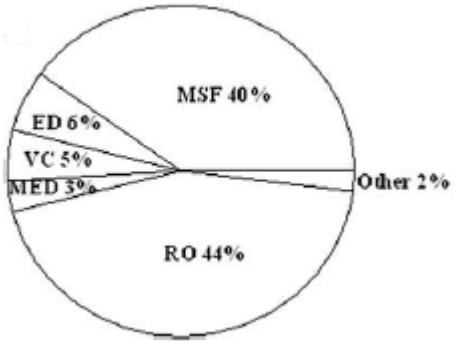

Figure 2: Distribution of desalination production capacity by process technology worldwide [4]

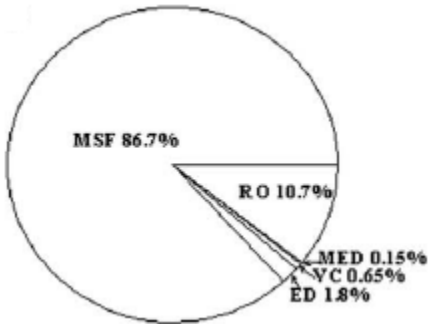

Figure 3: Distribution of desalination production capacity by process technology in the Middle East [4]

1.5.1 Multi-stage flash distillation. Multi-stage flash distillation (MSF) is a technology that was established in the early 1950s. MSF is the choice of technology for water desalination when a source of thermal energy is available or excess thermal energy is available. MSF is one of the technologies that could treat seawater with high dissolved solids to produce pure water. For instance, Arabian Gulf has total dissolved solids of 45,000ppm and MSF could produce distilled water with total dissolved solids (TDS) of

2 ppm. One of MSF process advantages is the vast experience in operation, design and maintenance. MSF unit can be 30,000m^3/day and as large as 70,000m^3/day according to [5].

The principle of MSF is to boil seawater in a number of stages in a closed vessel with progressively reducing pressure and to condense the water vapor to produce distilled water. Tracing the seawater path through the MSF unit, seawater intake enters the heat rejection section (HRJ) to cool and condense evaporating water. The seawater intake is then split into two, one portion is returned to the sea and the other portion is mixed with concentrated brine from the last stage. Circulating brine moves to heat recovery section (HRS) tubes in which brine gets heated up progressively. From HRS, brine moves to heat input section (HIS) tubes. In the HIS, brine is heated using steam. Brine leaving the HIS and enters HRS flashing chamber where water evaporates due to the vacuum created by an air ejector. Brine flows through multiple stages till it reaches the HRJ. From HRJ, brine, in addition to feed makeup, circulates again to HRS by the brine circulating pump. A portion of the concentrated brine is rejected to the sea to prevent the brine concentration ratio from exceeding 1.5. The flow of feed and product can be traced in the Figure 4.

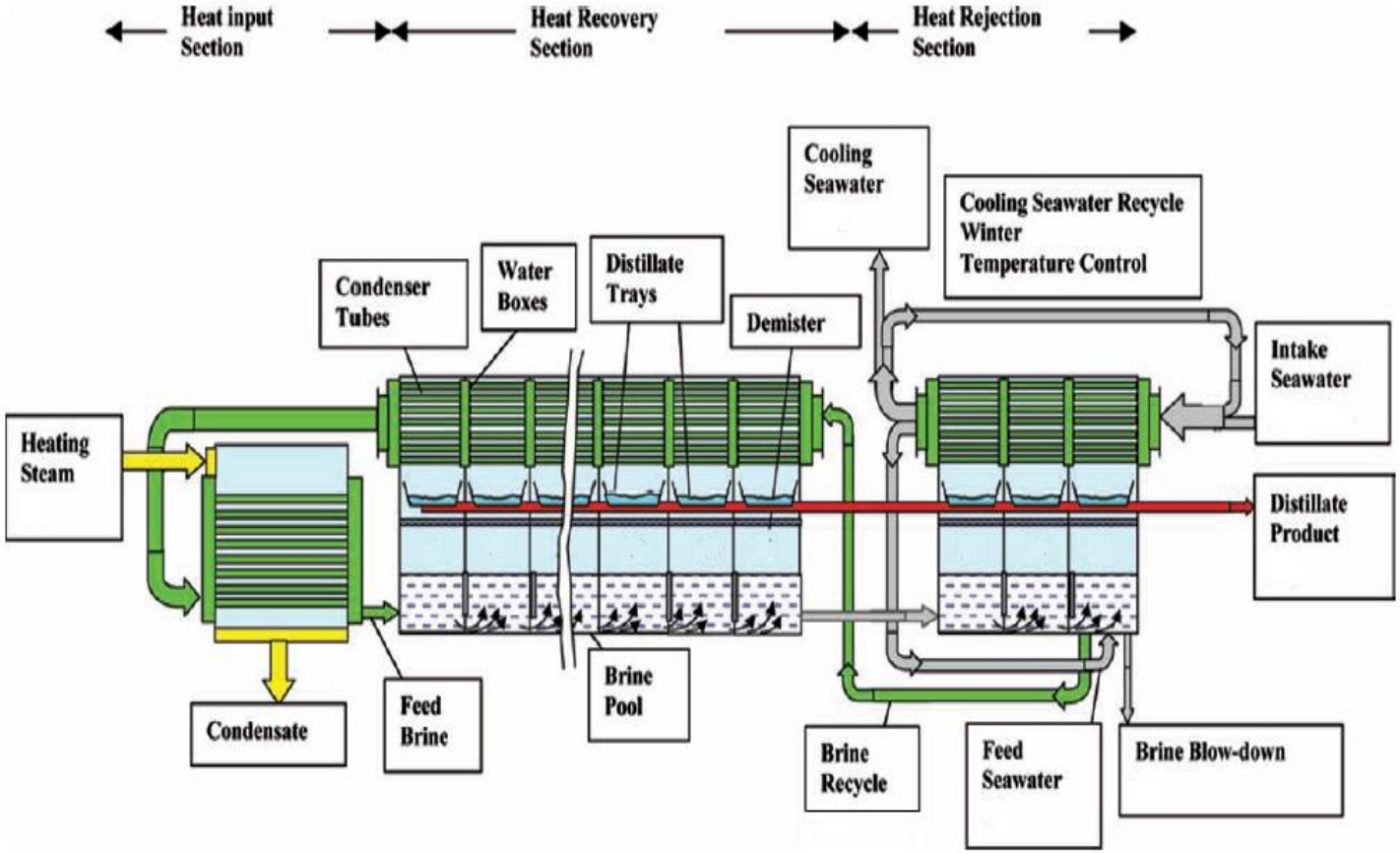

Figure 4: MSF schematic diagram [5]

The MSF process is limited by the maximum brine temperature in the HIS. The maximum brine temperature is 110-120°C by the threat of scaling, if this temperature is exceeded calcium sulfate scale forms. Calcium sulfate is hard scale that cannot be removed by chemical cleaning. Scale formation in HIS and HRS tubes reduces heat transfer coefficient causing a reduction on production. Antiscalant chemicals are usually added to reduce the scaling effect and extend continuous operation up to two years.

MSF advantages:

- It is a well-established technology and reliable
- The process is insensitive to feed concentration
- It produces high quality product
- Production cost is not affected by feed water salinity
- Requires minimal feed water pretreatment

MSF disadvantages:

- Energy intensive process
- Cannot operate below 70% of its design capacity
- Scale formation occurs at high operating temperature
- Concentrated brine disposal is considered an environmental impact
- High maintenance and operating costs

1.5.2 Reverse osmosis. Reverse osmosis (RO) was first introduced to the market in the 1960s using brackish water as feed [2]. With the continuous improvements in membrane design and technology, the RO market around the world is expected to reach $5.6 billion by the end of 2012 [6]. It also contributes to 40% of desalination installations worldwide.

The principle of RO comes from the osmosis process. Osmosis occurs when a fluid flows through a semi-permeable membrane from a low concentration fluid to a higher concentration fluid, diluting the second fluid. This process will equalize the fluid

concentrations. The membrane is selective in that it allows the flow of the fluid but rejects the solutes. Figure 5 demonstrates the process.

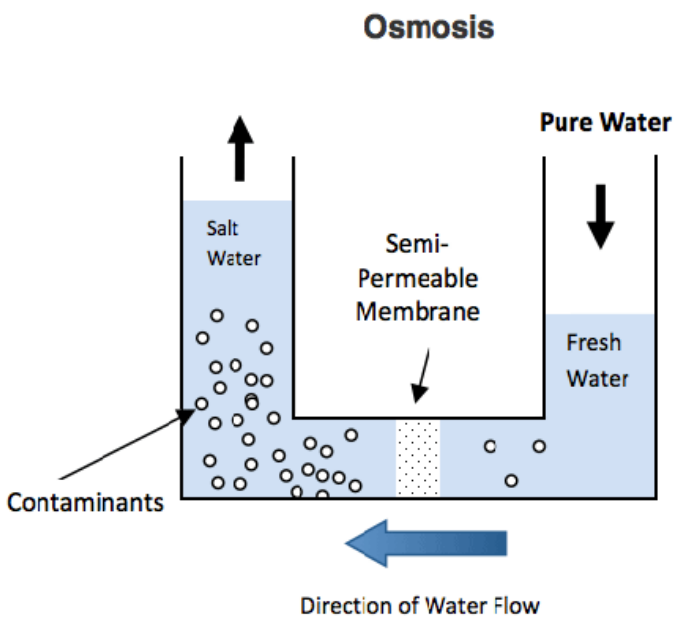

Figure 5: Natural Osmosis [7]

When the two solutions have the same concentration, equilibrium is reached. The height difference between the two fluids after equilibrium is called the osmotic pressure, seen in Figure 6.

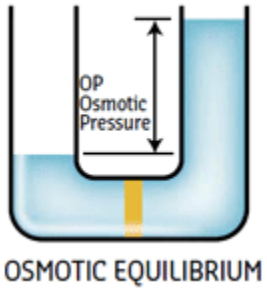

Figure 6: Osmotic pressure [7]

Reverse osmosis is simply applying external pressure to overcome the osmotic pressure and force the fluid to flow from a higher concentration to a lower concentration. In RO the feed flows with high pressure parallel to the membrane, the solute remains while the solvent passes through the membrane. The small membrane size allows it to remove small ions.

The most common RO membrane design is spiral-wound. The membrane is manufactured as a flat sheet and is spun around a center element which collects the pure product; the permeate. A series of membrane elements are placed in a pressure vessel in which feed enters from one side, concentrated feed or reject leaves from the other end. Membrane material is usually cellulose acetate, which can tolerate chlorine up to one ppm and does not attract ionically charged substances [8].

Cost implications associated with RO are high pressure feed requirements and routine membrane replacement. RO feed has to be at high pressure to overcome the osmotic pressure. As the RO process continues, the feed gets concentrated, resulting in an increase in osmotic pressure, therefore higher pressure is required for high recovery. Typical RO operating pressures are 5500 – 8000 kPa for seawater and 600 – 3000 kPa for brackish water RO [4]. It is estimated that RO requires 4 kW of electric energy per cubic meter, which contributes to approximately 1.8 kg CO_2 of pollution [9]. Compared to MSF, RO requires 25% less energy to produce a cubic meter of water.

Membrane fouling occurs because of water quality, such as dissolved solids, dissolved organics and biological material. It also reduces water flux. Since membranes have no obvious pores, fouling mechanism is usually surface fouling. The silt density index (SDI) is a measure of water fouling tendency, as the SDI increases the fouling rate increases. A well-developed pre-treatment scheme will reduce the SDI. Precipitation of contaminants from the feed water on the membrane is inevitable. The scaling process happens in three stages. The first and second stages are reversible, in which the ions begin to cluster and form nuclei. The third stage is irreversible in which salt crystals start to grow until it reaches the solubility limit. To reduce the precipitation from occurring, antiscalant chemicals are used. The chemicals disturb the nuclei formation or the

threshold of clustering [4]. Membrane scale and deposits can be removed by chemical cleaning, and restore water flux.

Membrane process advantages:

- Lower capital cost compared to distillation
- Operate at an ambient temperature which has lower scaling and corrosion potential compared to the thermal process
- Has high space/production capacity ratio

RO disadvantages

- Operates at high pressures
- Requires regular cleaning
- High membrane replacement cost

1.5.3 Limitations and environmental impact. Pre-treatment is an essential step in water desalination, either MSF or RO. However, RO requires extensive pre-treatment compared to MSF. Conventional pre-treatment processes are sometimes inadequate especially in the Middle East where turbidity, seasonal blooming and biological activities are high. These problems result in frequent cleaning and blocking of the membranes.

Desalination process environmental impact is a neglected aspect of the process. One of the most important emissions is brine discharge. The brine discharged back to the original source with three elemental differences, temperature difference, salinity gradient and chemical additives. In MSF distillation feed water is heated for pure water production, usually brine discharge temperature is regulated by the concerned authority not to exceed 5°C gradient compared to the original source. High discharge temperatures can lead to irregular dissolved oxygen concentrations affecting marine life. On the other hand, RO operates at atmospheric temperatures; therefore it is not associated with high

temperature discharge. Nevertheless, RO has a higher impact of discharge salinity. Brine discharge salinity is higher than the source, which may affect marine life in the long run. The third impact is chemical additive discharged with the brine. During the desalination process, chemicals, such as anti-foam, antiscalants and biocides, are added for different purposes and at different stages. These chemicals are carried with brine discharge affecting aquatic life.

1.6. Forward Osmosis

Although water desalination technologies have improved significantly throughout the years, desalination to produce fresh water cost is still too expensive for many countries. Therefore, desalination research and developments efforts have been extensive with the goal to make fresh water readily available at minimum cost. Forward osmosis is a technology available since the 1960s; though, it acquired greater interest only recently due to efforts to make forward osmosis processes commercially feasible and available.

Forward osmosis is a technology that takes advantage of the naturally occurring process of osmosis, in which fluid flows through a semi-permeable membrane from a low osmotic pressure to a higher osmotic pressure fluid. In FO, a draw solution with high osmotic pressure is required for water to permeate through a semi-permeable from the feed solution. The driving force in FO is the osmotic pressure gradient between the feed and draw solution.

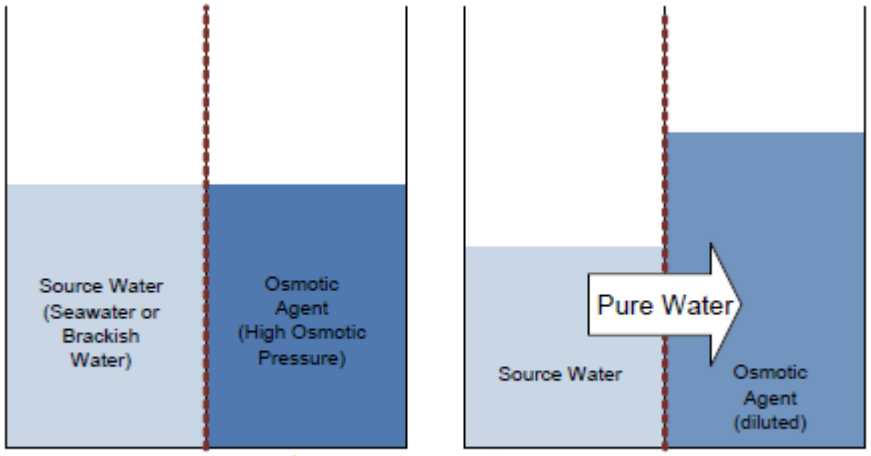

Figure 7: Forward osmosis [10]

FO is a promising technology because, compared to RO, it offers a water treatment method that requires low hydraulic pressure, high rejection and low membrane fouling. Although FO technology has been available since the 1960s [11], increasing energy costs and resources has led to the increasing interest in FO as a water treatment alternative. Despite different applications of FO similar challenges occur due to membrane ineffectiveness and effective draw solution selection. FO studies have mainly concentrated on membrane improvements and finding a draw solution that meets the process criteria. Figure 8 summarizes the expected advantages from the FO process.

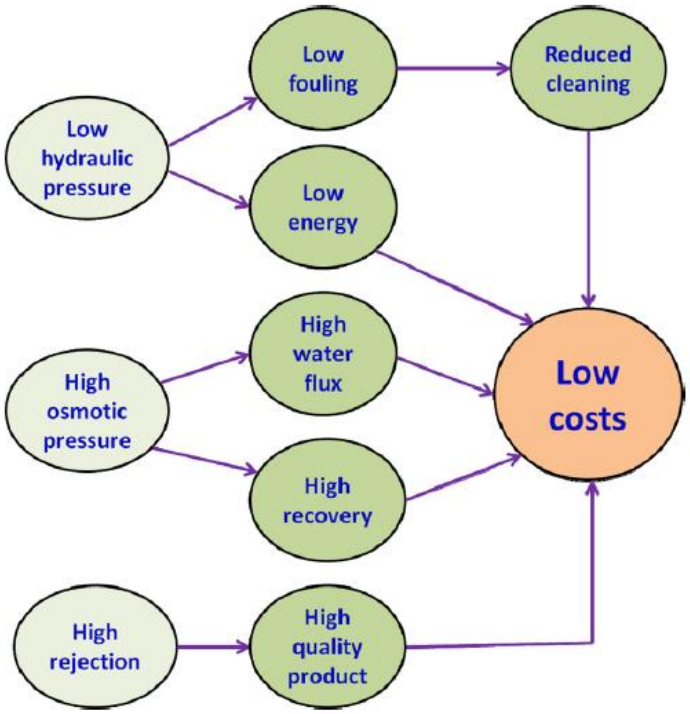

Figure 8: FO benefits summary [11]

1.6.1 Applications of osmotically driven processes forward osmosis (FO) and pressure retarded osmosis (PRO). FO and PRO are processes that depend on osmotic pressure gradient to achieve the required process. The main difference between FO and PRO is the membrane orientation. In FO process the feed solution is against the active layer of the membrane and draw solution is against the supportive layer. While in PRO process, the draw solution is against the active layer of the membrane and the feed solution is against the supportive layer of the membrane. The difference in membrane orientation affects the flux and the associated phenomena.

1.6.1.1 Power generation. Forward osmosis may be utilized for power generation based on salinity gradient. In a PRO process, the increase in the draw solution volume or pressure is used to rotate a turbine therefore generate electricity. Pressure retarded osmosis (PRO) operation is illustrated in the below figure. Seawater is the draw solution which is diluted with fresh water. Diluted seawater stream is split into two; one passes

through a pressure exchange unit to pressurize the seawater inlet, while the second stream passes through a hydro-turbine to generate power. Power generated using a PRO system depends on water flux and pressure deferential across the membrane.

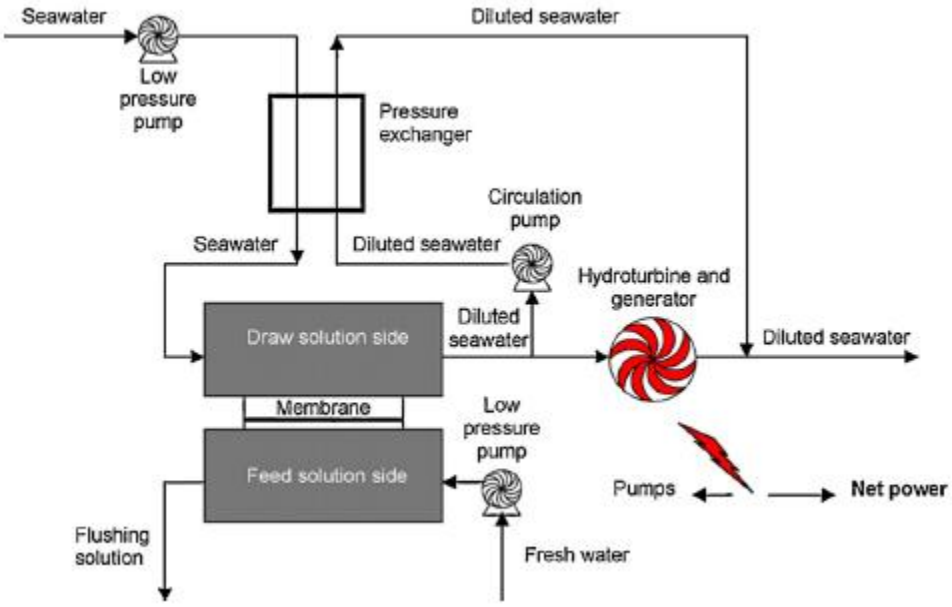

Figure 9: Schematic drawing of PRO power plant [12]

Some of the advantages of PRO are; it takes advantage of widely available resources, has a minimum impact on the environment, and is a renewable resource. PRO can generate a minimum of $4W/m^2$ of energy [11].

1.6.1.2 Desalination. Extensive studies have been conducted to utilize FO for water desalination to convert it from bench-scale to commercial use. The desalination process starts by the pre-treatment of the feed water, either seawater or brackish water, to remove large debris. The next step is the dilution of the draw solution by water permeate. The following step is the recovery of fresh water from the draw solution. The recovery method depends on the type of draw solution used. A bench-scale study has been conducted by [13] with seawater as feed solution and the draw solution used was a mixture of ammonium bicarbonate and ammonium hydroxide was used. The recovery method is to heat the draw solution mixture to 60ºC so that ammonia and carbon dioxide are released as gases and fresh water is retained. The ammonium carbonate mixture has

an osmotic driving force as a 127 bar [14] with seawater as feed. A pilot plant study was also performed by Hancock et al. [15] for the desalination of high salinity brine (TDS up to 77,000 mg/l) using ammonium carbonate as draw solution had a recovery of 66% and a flux of 2.6 l/m^2h.

Modern Water, UK was able to produce a commercial scale FO plant for water desalination. A pilot plant was first installed in Gibraltar, Mediterranean Sea in 2008. With a number of upgrades the facility has been operating since 2009 to provide drinking water for the surrounding area. Modern Water, UK, manufactured all membranes and the draw solution is its proprietary. The draw solution is recovered by a RO unit. A full scale FO plant was installed by the same company in Al Khaluf, Sultanate of Oman, with a design capacity of 100 m^3/day. The plant has a 30% seawater recovery with a product of TDS < 200 mg/l [10].

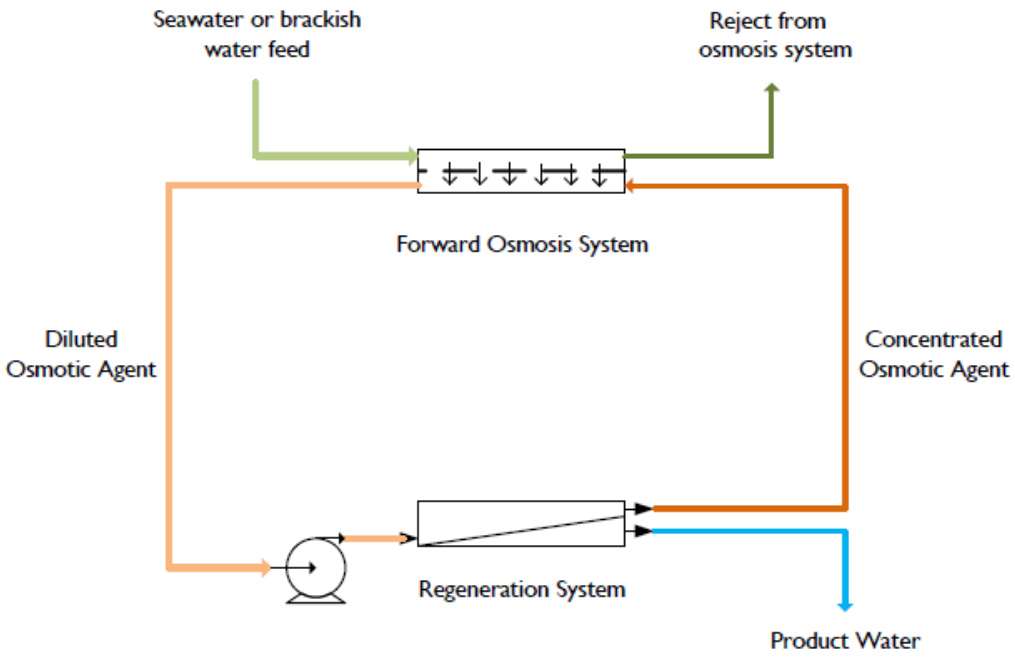

Figure 10: Typical FO desalination schematic diagram [10]

1.6.2 FO desalination limitation. Research in the field of forward osmosis processes has been dedicated to minimize or resolve the associated challenges. The main challenges are

- Concentration polarization,
- Draw solution development and separation, and
- Membrane development.

These challenges will be discussed in detail separately in the following sections. Being able to advance in these areas of FO process brings researchers one step closer to making forward osmosis commercially available.

1.7. Concentration Polarization in Osmotic Process.

FO process is driven by the difference in pressure across the membrane. Usually, the bulk osmotic difference is higher than the membrane osmotic difference. The reduction in osmotic pressure leads to reduction in flux. The reduction in flux is due to the two types of transport phenomena, internal concentration polarization and external concentration polarization.

1.7.1 Concentrative and dilutive external concentration polarization. In FO processes, the feed solution is against the active layer of the membrane, while the draw solution is against the membrane support layer. When water permeates through the membrane, solute accumulates over the membrane active layer. This results in higher feed concentration and a reduction in osmotic pressure. This phenomenon is referred to as concentrative external concentration polarization (ECP). On the other hand, draw solution against the porous support layer gets diluted as water permeates through. This phenomenon is referred as dilutive external concentration polarization. Both ECPs may be reduced by increasing fluid flow and turbulence. Compared to RO, ECP in FO is

regarded as minimum. Figure 11 below shows the effect of both dilutive and concentrative ECP.

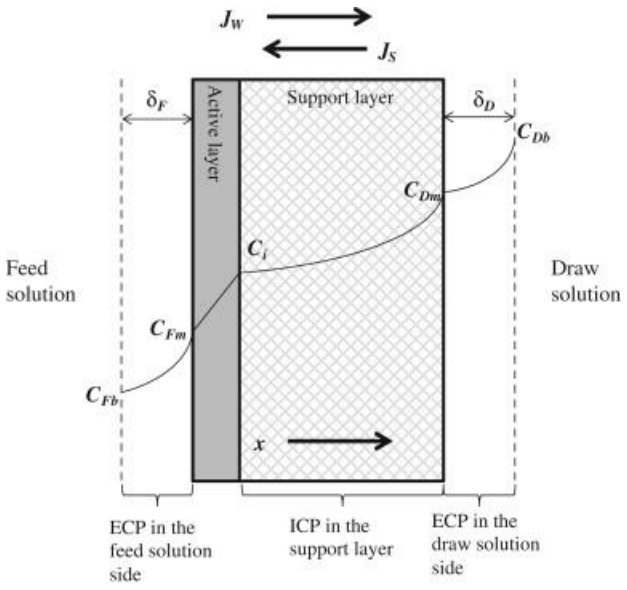

Figure 11: Concentrative and dilutive ECP [16]

To quantify the effect of concentrative ECP, the osmotic pressure at the membrane surface can be determined by the following equation:

$$\frac{\pi_{F,m}}{\pi_{F,b}} = \exp\left(\frac{J_w}{k}\right) \quad (1)$$

Where J_w is the experimental flux, k is the feed mass transfer coefficient, and $\pi_{F,m}$ and $\pi_{F,b}$ are membrane surface and bulk feed osmotic pressure respectively. All the modeling equations are according to McCutcheon [17] unless otherwise stated. The positive exponent indicates that membrane surface osmotic pressure is higher than the bulk osmotic pressure. The equation assumes that the ratio of feed membrane concentration to

feed bulk concentration is proportional to the osmotic pressure ratio. As for the effect of dilutive ECP it can be calculated by the following equation.

$$\frac{\pi_{D,m}}{\pi_{D,b}} = \exp\left(-\frac{J_w}{k}\right) \quad (2)$$

Where $\pi_{D,m}$ and $\pi_{D,b}$ are membrane surface and bulk draw solution osmotic pressure respectively. The negative exponent indicates a low membrane surface osmotic pressure compared to bulk draw solution osmotic pressure.

To model flux performance for FO process, the standard flux equation can be used which is valid for low flux with the assumption of no ECP.

$$J_w = A(\pi_{D,b} - \pi_{F,b}) \quad (3)$$

Where A is the water permeability coefficient and holds the assumption that no salt flows through the membrane. For high flux and taking into consideration dilutive and concentrative ECP, the flux should be modeled as,

$$J_w = A\left[\pi_{D,b}\exp\left(-\frac{J_w}{k_D}\right) - \pi_{F,b}\exp\left(\frac{J_w}{k_F}\right)\right] \quad (4)$$

Where k_D and k_F are the mass transfer coefficient of the draw and feed solutions respectively. The first term in the equation refers to the effect of dilutive ECP on the flux. The above equation is valid only for a dense membrane where both dilutive and concentrative occur simultaneously.

1.7.2 Concentrative internal concentration polarization. Asymmetric membranes are usually used in the FO process. In PRO processes feed solution is against the porous support layer and draw solution is against the active layer of the membrane. The feed flows easily through the porous layer, but it is more difficult for the water to permeate from the porous layer to the active layer. In this phase solute accumulates within the porous support layer, it is therefore called concentrative internal concentration polarization (ICP). To measure the severity of internal ICP the following expression is first used to determine the solute resistance to flow, *K* in PRO mode:

$$K = \left(\frac{1}{J_w}\right) ln \frac{B + A\pi_{D,m} - J_w}{B + A\pi_{F,b}} \quad (5)$$

In the above equation, B is the salt permeability coefficient of the active layer of the membrane. B can be estimated by the following equation:

$$B = \frac{(1-R)}{R} J_w \quad (6)$$

Where *R* is the characteristic performance of the membrane in RO according to Loeb [15]. While *K* is also defined as:

$$K = \frac{t\tau}{D\varepsilon} \quad (7)$$

Where *D* is the bulk diffusion coefficient of the solute, and τ, *t* and ε are tortuosity, thickness, and porosity of the membrane support layer. *K* is the resistance to solute diffusion within the membrane and can be considered as a measurement of how easy the solute diffuses through the support layer. Eq. 5 is used to estimate *K* based on experimental data when the membrane properties in Eq. 7 are unknown.

For membranes with high salt rejection, *B* can be neglected. Eq. 5 is rearranged to determine flux

$$J_w = A\left[\pi_{D,m} - \pi_{F,b}\exp(J_w K)\right] \quad (8)$$

In Eq. 8, $\pi_{D,m}$ is not a measurable quantity; therefore, it is replaced by $\pi_{D,b}$ determined by Eq. 2. Hence, the flux model with concentrative ICP and dilutive ECP, is:

$$J_w = A\left[\pi_{D,b}\exp\left(-\frac{J_w}{k_D}\right) - \pi_{F,b}\exp(J_w K)\right] \quad (9)$$

As for the concentrative ICP modulus to determine the feed solution osmotic pressure within the membrane layer the following equation is used.

$$\frac{\pi_{F,i}}{\pi_{F,b}} = \exp(J_w K) \quad (10)$$

1.7.3 Dilutive internal concentration polarization. Dilutive internal concentration polarization (ICP) is a phenomenon that occurs when draw solution is diluted by water permeate within the membrane support layer. The dilution of the draw solution results in the reduction in osmotic pressure therefore a decline in flux. Dilutive ICP is one of the leading factors of limited progress in FO membranes, as the membrane has to have the least ICP with no salt leakage. The governing model of dilutive ICP is as follows

$$K = \left(\frac{1}{J_w}\right) ln \frac{B + A\pi_{D,b}}{B + A\pi_{F,m} + J_w} \quad (11)$$

Where $\pi_{F,m}$is calculated using Eq. 1. As for the draw solution osmotic pressure within the membrane, it can be calculated from the below equation:

$$\frac{\pi_{D,i}}{\pi_{D,b}} = \exp(-J_w K) \quad (12)$$

Where $\pi_{D,i}$is the draw solution osmotic pressure within the active layer and support layer interface. It can be observed also that the internal osmotic pressure is less than the bulk osmotic pressure leading to a reduction in the driving force. To model flux with dilutive ICP the following equation is used

$$J_w = A\left[\pi_{D,b}\exp(-J_w K) - \pi_{F,b}\exp\left(\frac{J_w}{k}\right)\right] \quad (13)$$

The model assumes asymmetric membrane with dilutive ICP coupled with concentrative ECP.

For all cases ECP and ICP contribute negatively to the process and results in reduction of flux and overall driving force. It also implies that an infinite increase in osmotic pressure will have a diminishing effect on flux increase.

1.8. Draw Solution Types and Selection

Selecting the appropriate draw solution for the FO process is very critical since it is the driving force in the process. Most importantly, the draw solution has a higher osmotic pressure than the feed solution. Various solutions have been considered as draw solution based on experimental trials [10, 13, 18]. Figure 12 shows the osmotic pressures of different draw solutions at range of concentrations. To generate higher osmotic pressure the draw solution solute has to be highly soluble in water. It can be seen from Figure 12 that for most draw solutions, increasing the concentration infinitely has a dimensioning effect over the osmotic pressure. The osmotic pressure in this figure was determined using the OLI stream analyzer 2.0.

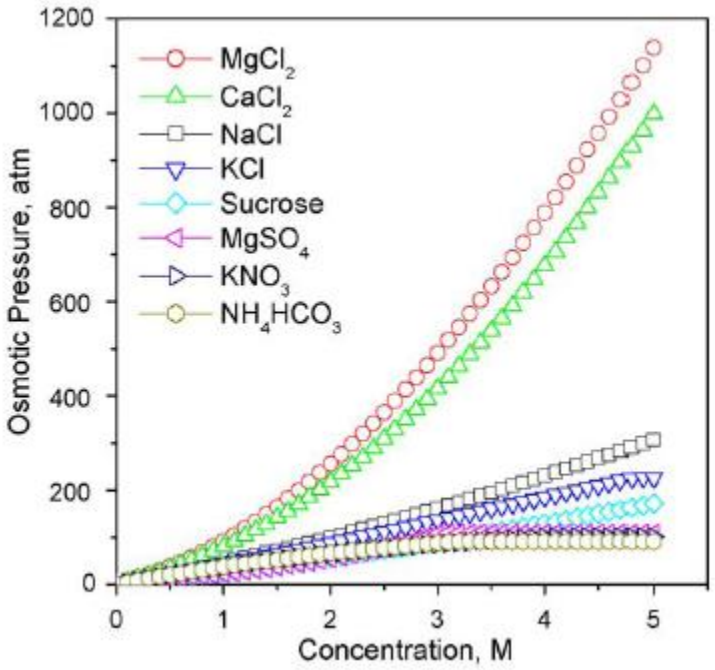

Figure 12: Osmotic pressure as a function of concentrations of various potential draw solutions [14]

The second most important criterion of the draw solution is that it can be easily recovered from the product water. A process to regenerate the draw solution is very important because it is the step at which the feed is recovered and the possibility to recycle the draw solution is an added benefit. To keep in consideration, the draw solution also has to be non-toxic, non-reactive with the membrane and economically feasible to recover.

One of the most used draw solutions in the FO desalination process is a mixture of ammonia and carbon dioxide gases at different ratios. This draw solution results in high flux and recovery. One benefit of this draw solution is its ease of separation from the permeate. The draw solution is heated to 60ºC to release ammonia and carbon dioxide gas, while the product remains. Other draw solutions that have been tried are sulfur dioxide, aluminum sulfate, glucose, fructose, and NaCl solution. NaCl is often used as a draw solution because it is highly soluble and the possible recovery from the product by RO.

A draw solution selection criteria method adopted from Achili [18] which was developed to select an inorganic draw solution. Figure 13 shows the draw solution selection method. Measuring hazardous materials are classified according to the Hazardous Material Identification system (HMIS). It classifies chemicals based on their health, flammability and physical hazards

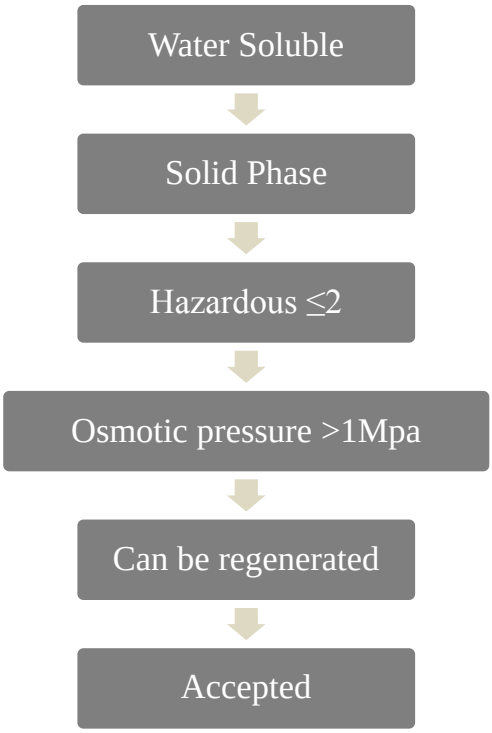

Figure 13: Flow diagram for draw solution selection

The draw solutions selected for the thesis is magnesium sulfate ($MgSO_4$) and copper sulfate ($CuSO_4$). Both salts are highly soluble in water, non-toxic and separable from the feed solution. $MgSO_4$ has a maximum solubility of 342 g/l [18] and $CuSO_4$ has a maximum solubility of 220,000 ppm [19] at 25°C. Both draw solutions can be recovered by metathesis precipitation reaction. A metathesis precipitation reaction is a reaction in which cations and anions exchange partners and the product of the reaction is insoluble solid.

$$AX_{(aq)} + BY_{(aq)} \rightarrow AY_{(s)} + BX_{(s)} \quad (14)$$

Both draw solutions can react with barium hydroxide for solid precipitants. The advantage of magnesium and copper sulfate as draw solutions over other draw solutions is the elimination of thermal energy use to recover the draw solution.

1.9. Forward Osmosis Membrane

In general, any non-porous selectively permeable membrane can be used for an FO process. Earlier FO investigations used RO membranes which were designed for a pressure driven process. In the 1960s Loeb and co-workers were the first to develop a membrane especially designed for FO and PRO processes. Membranes are usually characterized by their salt rejection and flux rate. In addition membranes should maintain the following properties

- Low fouling propensity
- Chlorine resistance
- Chemical stability toward draw solutions
- Minimum reverse osmosis
- Tolerate mechanical stress

Whether commercially available or a custom made membrane, all are made with the aim to maintain all the above properties.

1.9.1 Membrane types. Forward osmosis membranes are usually asymmetric membranes composed of a thin selective layer and a porous mechanical support layer. Another FO membrane type is the thin film composite (TFC) membrane. It is made up of polymer layer supported by a porous layer. The support layer in both cases acts as a boundary layer that limits the membrane performance. Some of the membrane materials of construction are:

- Cellulose acetate (CA)
- Polybenzimidazole (PBI)
- Polysulfone and polyethersulfone (PSf)
- Polyamide (PA)
- Poly(amide-imide) (PAI)

Each of the above materials has special properties that would make it suitable for membrane construction properties, such as temperature resistance, mechanical properties, hydrophilic nature and wetting [20].

1.9.2 Selected membrane. Studies throughout the years investigated different membrane types either commercially available or in-house constructed. CA membranes have been extensively used since it was first developed. In addition, the first commercially available FO membrane was CA membrane by Hydration Technologies Inc. (HTI) in the 1990s. Cellulose acetate is used in membrane construction because of its smoothness, sturdiness and hydrophilic nature. The hydrophilic nature of the membrane increases wetting therefore reducing ICP and increases flux. Cellulose acetate based membranes have been studied by Sairam [21] in which methods of membrane preparation are investigated. While Su et al [22] examines the properties of a fabricated cellulose acetate membrane.

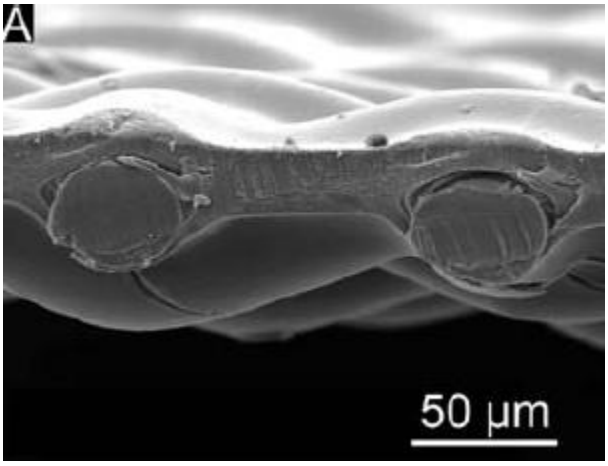

Figure 14: Cross section SEM image of HTI membrane [19]

The HTI cellulose acetate (CA) membrane is selected for the thesis. The reason of selection is because it has been reported to give higher water flux [13]. Figure 14 is a cross section SEM image of the HTI membrane. The membrane thickness is less than 50

μm. The HTI CA membrane is embedded with a polyester support mesh thicker than commercial composite membranes. CA selective layer is 10-20 μm, which is thick compared to thin film composites (TFC). On the other hand, CA membranes are hydrophilic, which makes it unlikely to foul compared to other hydrophobic membranes.

Chapter 2: Methodology

2.1. Experimental Setup

The bench-scale experiments were conducted to determine water flux at different feed concentrations and draw solution types. The apparatus was a circular U-tube as shown in the figure below.

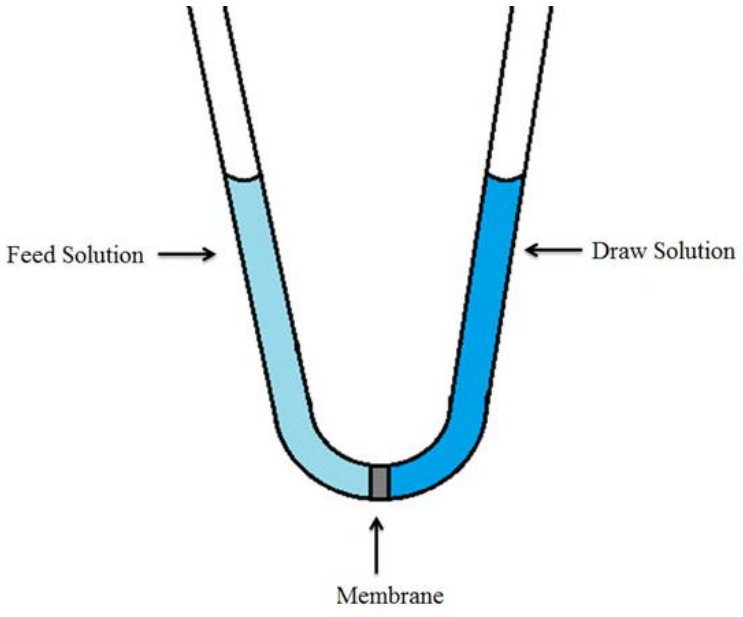

Figure 15: U-tube apparatus

The CA membrane from HTI was placed in the middle of the tube to separate the feed and draw solutions. Equal quantities of feed and draw solutions were placed in the tube to ensure equal hydraulic head. The feed was placed against the active side of the membrane, while the draw solution was placed against the support layer. The tube was

graduated and calibrated to measure changes in volume occurring due to the natural process of osmosis.

2.2. Materials and Methods

All chemicals used in the experiments were of analytical grade and used without further purification. All solutions were prepared with deionized water with <50 ppm TDS. The feed solution was prepared using analytical grade NaCl purchased from Fisher Scientific, UK. One draw solution was prepared using analytical grade magnesium sulfate heptahydrate ($MgSO_4.7H_2O$) purchased from Merck Group, Germany. While the other draw solution was prepared using analytical grade copper sulfate pentahydrate ($CuSO_4.5H_2O$) purchased from BDH Laboratory Supplies, UK.

2.3. Experimental Procedures

All experimental trials were conducted at a temperature of 25±3ºC and the following procedure was followed:

- The apparatus was cleaned prior to every trial to ensure no salts or deposits were present.
- When the membrane was connected, a leak test was done to ensure proper fixing.
- The tube was filled with equal amounts of feed and draw solution on designated side of the tube.
- The change in volume was measured after appropriate time intervals.
- The feed concentration was measured during the designated time intervals with a TDS meter.
- The final draw solution concentration was measured using a gravimetric analysis method.

2.4. Experimental Flux Calculation

Using the experimental setup and conditions described earlier, volume change was used to determine flux using the following equation [23]:

$$J_w = \frac{\Delta V}{A_m \Delta t} \quad (15)$$

Where ΔV is the measured change in volume, A_m is area of the membrane and Δt is the change in time.

2.5. Flux Modeling

To predict the water flux, steps shown in Figure 16 were followed with the required parameters.

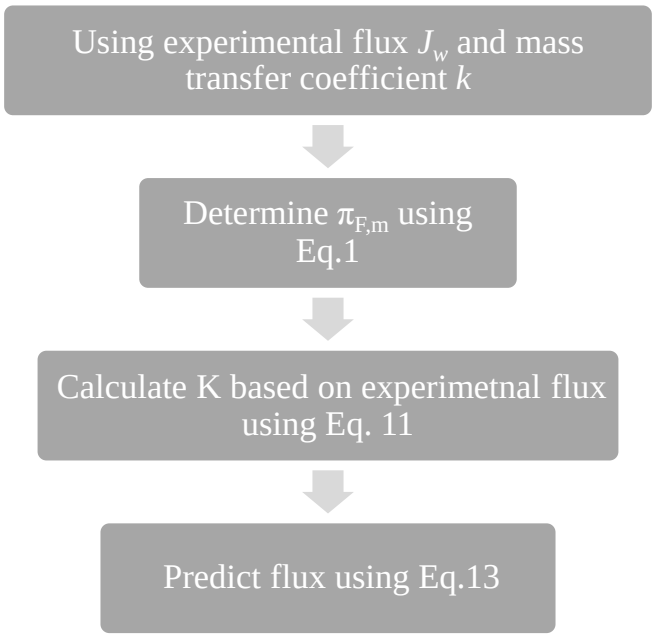

Figure 16: Flux modeling procedure

The equation selected for flux modeling is Eq. 13 mentioned earlier

$$J_w = A\left[\pi_{D,b}\exp(-J_w K) - \pi_{F,b}\exp\left(\frac{J_w}{k}\right)\right] \quad (13)$$

The equation is in terms of

- A water permeability coefficient
- k mass transfer coefficient
- $\pi_{D,b}$ bulk draw solution osmotic pressure
- $\pi_{F,b}$ bulk feed solution osmotic pressure
- K solute resistance to diffusion

Each of the above parameters must be determined to predict flux. Table 1 shows a typical set of parameters that were used in the calculation.

Table 1: Flux calculation parameters

Salt permeability coefficient of the active layer (*B*) [24]	**1.27E-07 m/s**
Water permeability coefficient (*A*) [25]	**3.125E-07 m/s·atm**
Feed mass transfer coefficient (*k*) [17]	**1.74E-05 m/s**
Effective membrane area (A_m)	**6.157cm^2**

The osmotic pressure of a solution can be calculated by the following Van Hoff equation which is applicable for very dilute solutions [26].

$$\pi = \left(\frac{n}{V}\right) RT \quad (16)$$

Where $\left(\frac{n}{V}\right)$ is the molar concentration of a solute in a solution. Osmotic pressure may also be determined using the following viral equation.

$$\frac{\pi}{cRT} = 1 + Bc + Cc^2 + Dc^3 + \cdots \quad (17)$$

Where (*B, C, D*…) are viral coefficients which are usually determined empirically by fitting experimental data of osmotic pressures to the equation. To determine the viral coefficients of all solutions at different concentration, many experimental data are required. Therefore, an alternative method of determining the osmotic pressure is needed. the osmotic pressure was measured using OLI Systems Inc. (Morris Plains, NJ) and Aspen HYSYS (Cambridge, MA) software.

2.5.1 HYSYS and OLI interface. Aspen HYSYS is a process modeling and simulation tool for conceptual design. Aspen Tech was founded by a chemical engineering professor at MIT in 1981. The purpose of the program was to store process design information in the form of models for more efficient data retrieval. HYSYS has built-in property packages that provide accurate predictions of thermodynamic, physical and transport properties over a wide range of chemicals. HYSYS relies on experimental data from reliable sources to develop thermodynamic models. The experimental data base has more than 1500 components and 16,000 fitted binaries.

The environment basis is a concept in HYSIS that allows the use of the built-in thermodynamic data. In the Simulation Basis Manger, the required components and the fluid package are selected. The Simulation Basis Manger can be re-entered at any stage of the modeling process to perform changes in the components and fluid package. The

fluid package contains all the required properties of pure components. Various types of property packages are available depending on the application which include; equations of state, activity models, and vapor pressure models. The property package of concern for forward osmosis analysis is the OLI-Electrolyte. The package is designed to predict properties of water solutions. OLI-Electrolyte package is designed by OLI Systems software.

The OLI software enables the determination of electrolyte properties that cannot be provided by HYSYS such as ionic strength, specific electrical conductivity, molar electrical conductivity, and osmotic pressure. It also enables modeling of complex chemical phenomena including inter-phase equilibria between vapor, aqueous and solid phases. The electrolyte systems calculations are based on Helgeson equation of state for standard thermodynamic properties, Bromley-Zemaitis for excess properties and Pitzer and Setschenow for excess properties of molecular species.

To demonstrate the accuracy of the OLI prediction, Figure 17 is a plot of predicted and observed solubility data [27].

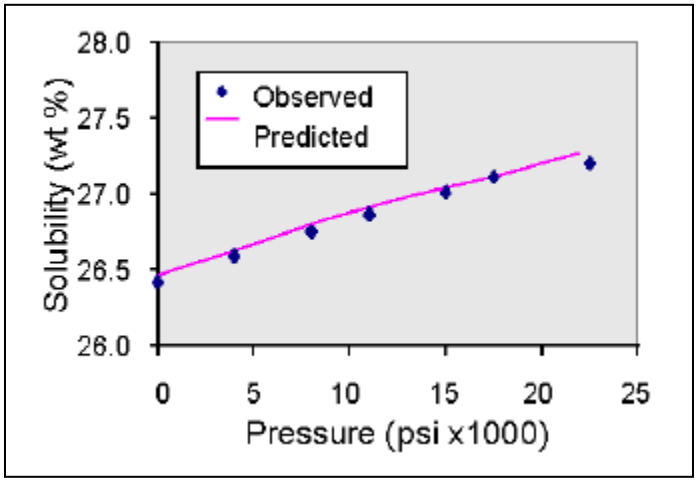

Figure 17: Solubility as a function of pressure [27]

Figure 17 compares the observed solubility and predicted solubility using the HYSYS Electrolyte OLI package at various pressures. The graph shows the predicted solubility of NaCl versus pressure is in agreement with the observed solubility.

Another example to show the accuracy and capabilities of OLI software is a sour water system composed of ammonia, hydrogen sulfide, carbon dioxide, and water. Vapor-liquid equilibrium (VLE) reaction and reaction in the aqueous phase occurs in the system. Partial pressure of ammonia, hydrogen sulfide, and carbon dioxide were determined using a vapor-liquid equilibrium model and compared to experimental data. The results are shown in Figure 18.

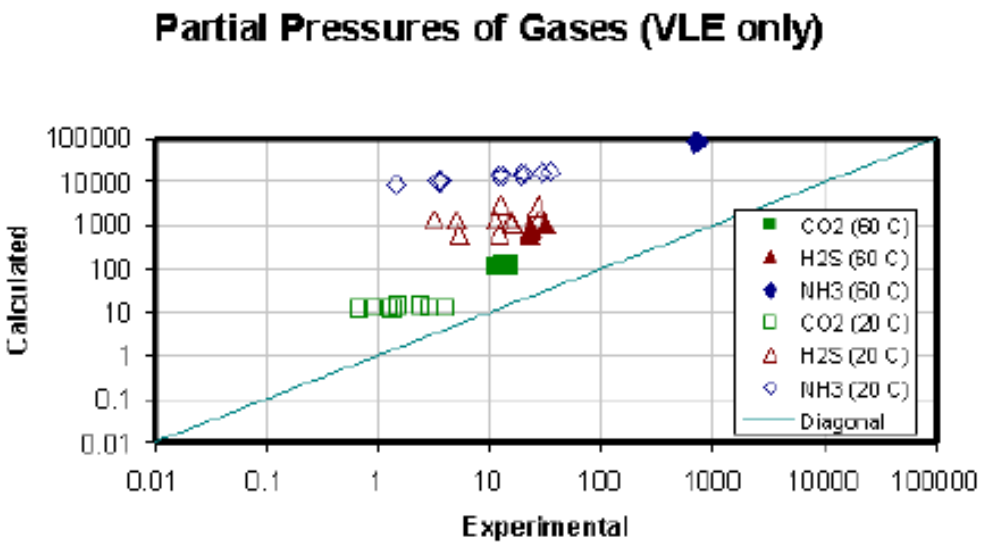

Figure 18: Calculated versus experimental partial pressure (VLE model) [27]

The calculated partial pressure exceeds the actual partial pressure. The model used for partial pressure calculation does not take into consideration aqueous reactions

and speciation. Furthermore, the experimental data were compared to partial pressure predicted using the OLI model and the results were as follows.

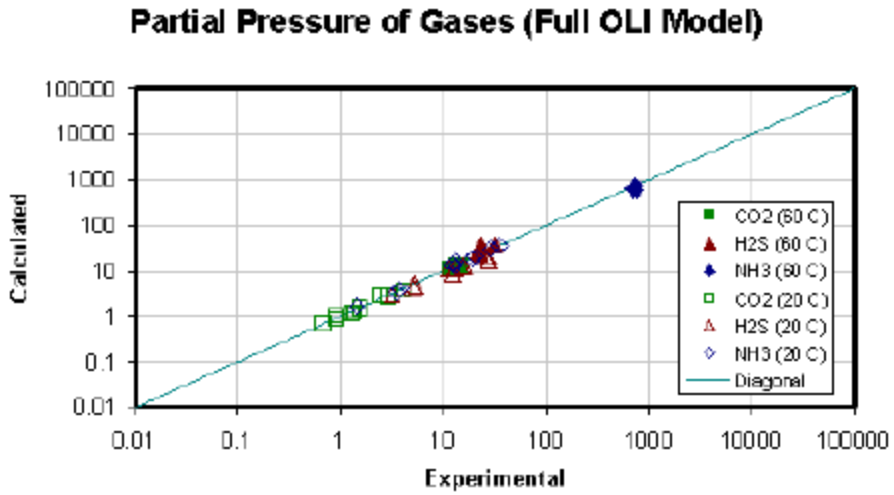

Figure 19: calculated versus experimental partial pressure (OLI model) [27]

The OLI model gives a good prediction of the partial pressure with the aqueous phase reactions. The model agrees with the actual partial pressure over various concentrations of the components in the system.

OLI software and Aspen HYSYS are also capable of determining the osmotic pressures of the feed and draw solutions that are used to model the flux. A sample data are shown in Table 2.

Table 2: Osmotic pressure data

Feed Solution	Concentration	Osmotic pressure
Brackish water	5,000 ppm NaCl	396 kPa
Sea water	40,000 ppm NaCl	3,217 kPa
Draw solution	**Concentration**	**Osmotic pressure**
Magnesium Sulfate	240,000 ppm $MgSO_4$	5,534 kPa
Copper Sulfate	200,000 ppm $CuSO_4$	2,700 kPa

2.5.2 Process Parameters. To model the flux, the solute resistance to diffusion (*K*) must be determined. The membrane used in this work was obtained from HTI (Albany, OR). The membrane properties are proprietary therefore parameters required to determine *K* are not available. On the other hand, *K* can be calculated based on experimental data using Eq. 11.

$$K = \left(\frac{1}{J_w}\right) ln \frac{B + A\pi_{D,b}}{B + A\pi_{F,m} + J_w} \tag{11}$$

Where *B* is the salt permeability coefficient which is equal to 1.27E-07 m/s [24]. In addition, $\pi_{F,m}$ may be determined using Eq. 1. To predict the flux, an average value of *K* was used in each run.

Once all required parameters to calculate the flux are available, the flux can be predicted. Eq. 11 is an implicit equation in terms of flux, hence, to solve the nonlinear equation, Newton's method was used, [28].

$$x_{i+1} = x_i - \frac{f(x_i)}{f'(x_i)} \tag{18}$$

In which Eq. 18 is repeatedly applied until either one or both of the conditions below converge.

$$|x_{i+1} - x_i| \leq \varepsilon_1 \; and/or \; |f(x_{i+1})| \leq \varepsilon_2 \tag{19}$$

To apply Newton's method, the selected model must equal zero and the derivative has to be determined. When applying Newton's method to the flux model x_i will be J_w, while $f(J_w)$ and $f'(J_w)$ are as follows.

$$f(J_w) = A\left[\pi_{D,b}\exp(-J_w K) - \pi_{F,b}\exp\left(\frac{J_w}{k}\right)\right] - J_w \tag{20}$$

$$f'(J_w) = A\left[-K\pi_{D,b}\exp(-J_w K) - \frac{\pi_{F,b}}{k}\exp\left(\frac{J_w}{k}\right)\right] - 1 \tag{21}$$

Once $f(J_w)$ and $f'(J_w)$ are calculated, J_w may be determined using the below equation.

$$J_{w,i+1} = J_{w,i} - \frac{f(J_w)}{f'(J_w)} \tag{22}$$

Chapter 3: Results and discussion

3.1. Initial Membrane Performance

The first stage of conducting FO experiments was to test the membrane performance. Deionized water with 50 ppm TDS was used as a feed solution, whereas the draw solution was 8,000 ppm NaCl solution. 500 ml of the feed was placed against the active layer of the membrane and 500 ml of the draw solution was placed against the membrane support layer. The change in volume of feed solution and draw solution concentration were recorded at different time intervals. It was observed that as the draw solution concentration decreased, the flux decreased. Figure 20 shows the flux as a function of draw solution concentrations.

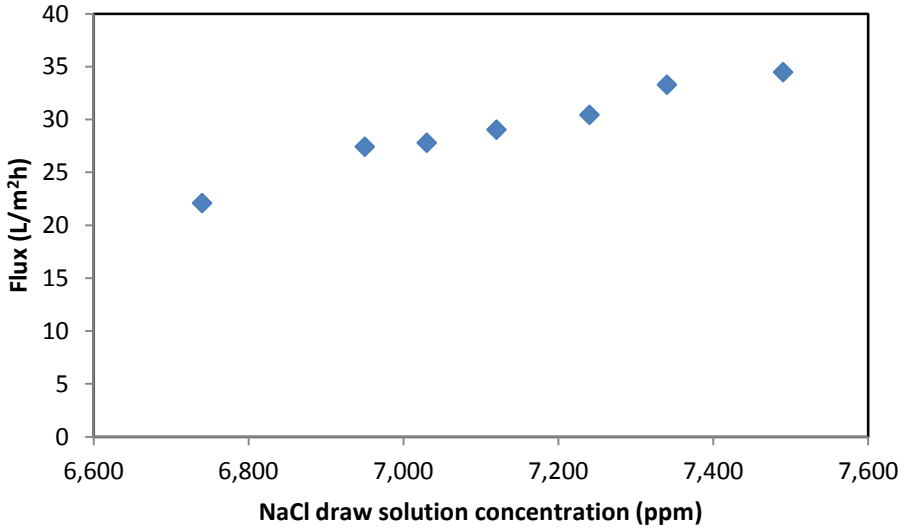

Figure 20: Flux as a function of draw solution concentration, membrane basic performance

As expected, the result showed as the draw solution concentration reduces, so did its osmotic pressure, reducing the overall driving force.

3.2. Flux Modeling with NaCl as Draw Solution

Many runs were carried on to determine the flux at different feed concentrations. The feed solution concentration was varied from 5000 ppm to 40,000 ppm NaCl solution. For those runs, the draw solution was 80,000 ppm NaCl solution. The runs gave an insight of the expected experimental flux compared to the flux calculated by Eq.3 with the assumption that flux is a function of the difference in osmotic pressure, see Figure 21.

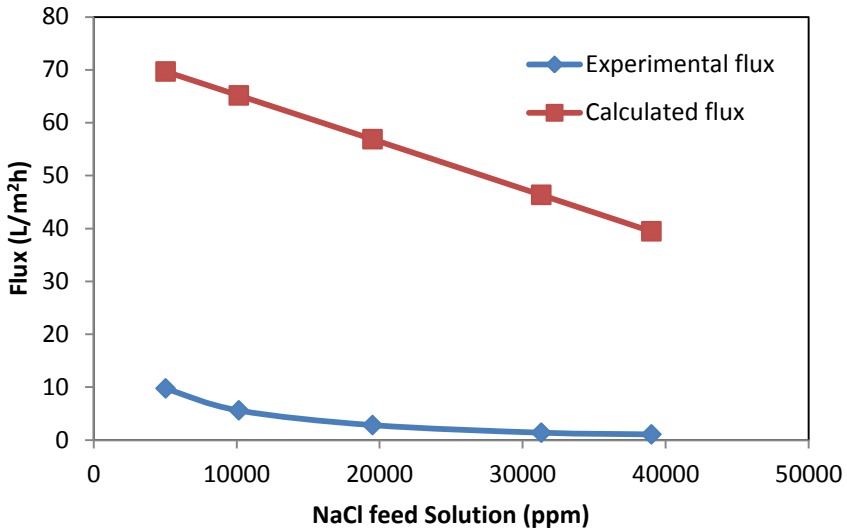

Figure 21: Flux as a function of feed concentrations, experimental and calculated flux

Figure 21 clearly shows that the calculated flux using Eq.3 (without including ECP or ICP) over estimates the measured flux in the process. It also assumes a linear relationship between flux and osmotic pressure difference. Figure 21 also shows the importance of both transport phenomena on flux in FO processes. It is observed that a

drop in flux occurs as the feed concentration is increased. A maximum of 40,000ppm NaCl solution was chosen to represent sea water concentration.

Moreover, flux modeling using Eq.13 that takes into consideration concentrative ECP and dilutive ICP, was performed. The model assumed concentrative ECP and dilutive ICP occurring simultaneously for as asymmetric membrane. The model results were compared to experimental data, see Figure 22.

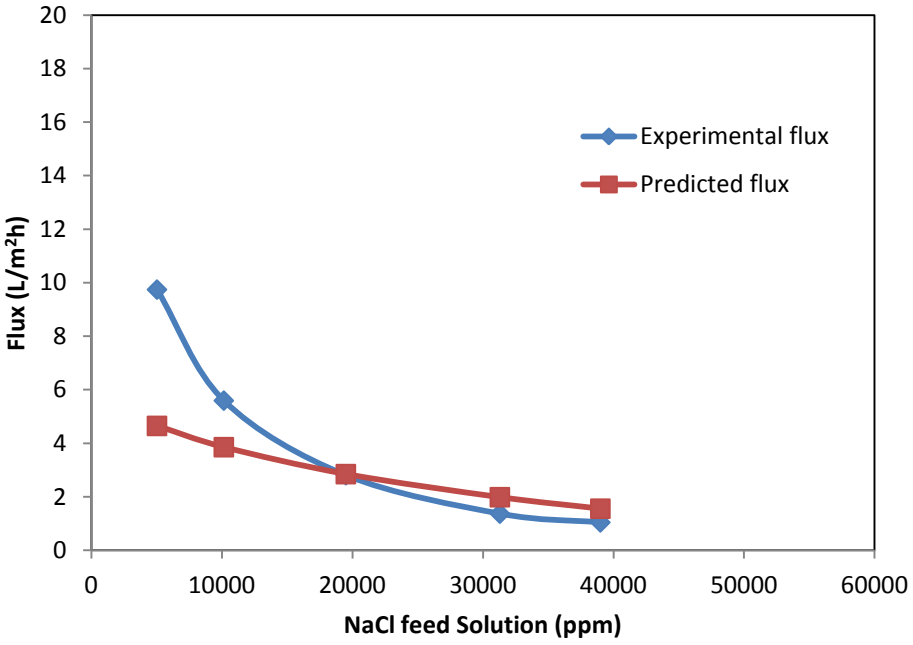

Figure 22: Flux as a function of feed solution concentration for experimental and predicted flux

The flux prediction model contains solute resistance to flow (*K*), which is calculated from experimental results since *K* is not known. At high feed concentrations, the model has a good agreement with the experimental results. Nonetheless, the model failed to accurately predict the flux when the feed has a low salt concentration (5000 ppm) as shown if Figure 22.

3.3. Verification of the Flux Mode

To examine the accuracy of the water flux model, the results were tested against measurements of other researchers [13, 17, 22, 29, and 30]. Most of them were conducted on forward osmosis processes in which the feed solution was against the active layer of the membrane and the draw solution was against the supportive layer. Flux model parameters had to be re-evaluated and/or estimated for each data set as it was illustrated in section 2.5.

G.T Gray et al. [29] study was carried out to determine the effect of membrane orientation on ICP in a forward osmosis process. The study was conducted using solutions with different molecular weights, various membrane orientation, and variable feed and draw solutions concentrations. Their membranes were obtained from Hydration Technologies (Albany, OR) which were believed to be a cellulose acetate membrane with asymmetric structure. The test unit was a modified SEPA cell from GE Osmonics (Trevose, PA). The feed and draw solutions flow co-currently in a closed loop circuit. The temperature of the feed and the draw solutions were maintained at 22.5±1.5ºC via a constant temperature bath. Maintaining a constant temperature ensures a constant mass transfer coefficient over the duration of the run. The water flux was calculated by measuring the rate of change in draw solution weight.

The model was tested against the water flux measurement of G.T Gray et al. [29] where both the feed and the draw solutions were NaCl solutions. As for the flux model parameters, the water permeability coefficient, *A*, was given as 0.027 m/atm-day and the solute permeability coefficient, *B*, was given as 0.011 m/day. The dimensions of the test unit were not stated in the study; therefore, the mass transfer coefficient could not be calculated. On the other hand, the study clearly mentioned that flow was turbulent which indicated a high mass transfer coefficient and minimum external concentration polarization. An estimated mass transfer coefficient (*K*) was used. As it was outlined earlier in Figure 15, solute resistance to flow, *K*, was calculated first from each data point. The average solute resistance, *K*, was then used to determine the flux. The results were shown in Figure 23.

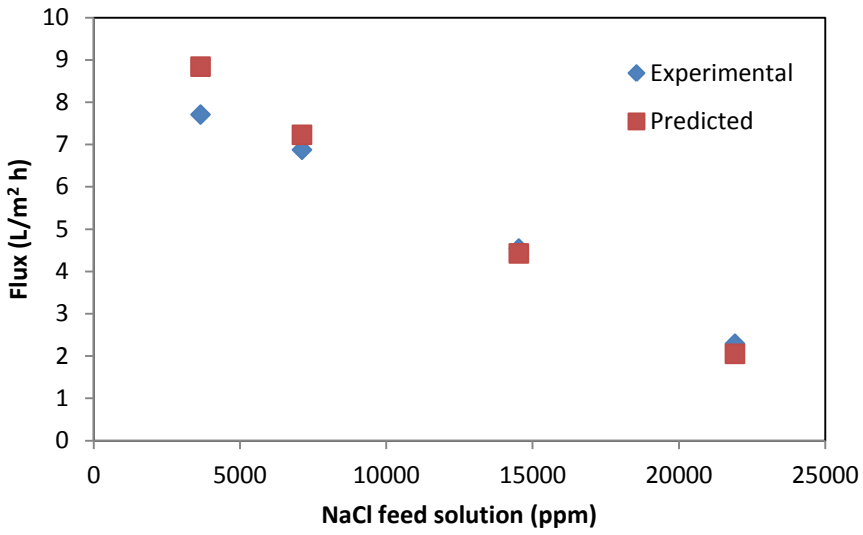

Figure 23: Flux as a function of feed solution concentration, data from G.T. Gray et al. [29]

Figure 23 shows water flux as a function of feed solution concentration for both experimental and predicted flux data. As expected, as the feed solution concentration increases the water flux decreases. Figure 23 shows an excellent agreement between observed and predicted flux. It is also observed that the model has a good agreement even at low water flux. Based on this excellent agreement, the model (with the solute resistance to diffusion) can be used to optimize the process and the apparatus. Furthermore, it was concluded the chosen mass transfer coefficient did not affect the predicted water flux which confirms a low concentrative external concentration polarization. For the system above, dilutive ICP was the governing phenomena of the flux model.

J. Su et al. [22] fabricated a cellulose acetate nano-filtration hollow fiber membrane and tested it for the forward osmosis process. Their study was an attempt to fabricate a membrane for forward osmosis process with high performance compared to commercially available cellulose acetate membranes, in terms of flux. The fabrication process of the membrane was called dry-jet, wet-spinning process. The membrane fabrication started by drying cellulose acetate powder in a vacuum oven then mixing it with acetone and formamide with known concentrations. This mixture to create the

membrane selective layer was called the dope solution. The mixture to create the porous support was called the bore fluid. It was a mixture of N-mthyl-2-pyrrolidone (NMP) and water. The two fluids were extruded through a syringe pump to create the hollow fibers. The fibers were immersed in water for few days then soaked in glycerol solution. Finally, they were made into membrane modules.

The selected performance data from J. Su et al. [22] study was from a group of membranes designated as CA-#3. CA-#3 membranes passed through a heating process. The membranes were first heated in a water bath at 60ºC for 60 min then rapidly cooled. The second stage was to heat the membranes to 95ºC for 25min then rapidly cooled. The heat treatment modified the selective layer morphology and the support layer structure. The working feed solution was deionized water which was assumed to have zero osmotic pressure. The draw solution was a magnesium-chloride solution with various concentrations. In the test unit, feed and draw solutions were circulated counter currently through the membrane modules. Water flux was determined by the weight change of the draw solution.

The steps in Figure 15 were followed to model the flux measurement of J. Su et al. [22] study. The concentrations and osmotic pressures of the draw solution were also reported by J. Su et al. [22]. The water permeability coefficient, *A*, of CA-#3 membranes was 0.47 L/m^2bar h. The Solute permeability coefficient was assumed to be zero due to the low salt leakage. The average solute resistance to diffusion, *K*, was calculated to be 3.11E6 s/m; accordingly the water flux was calculated. The results of the water flux data modeling is shown in Figure 24.

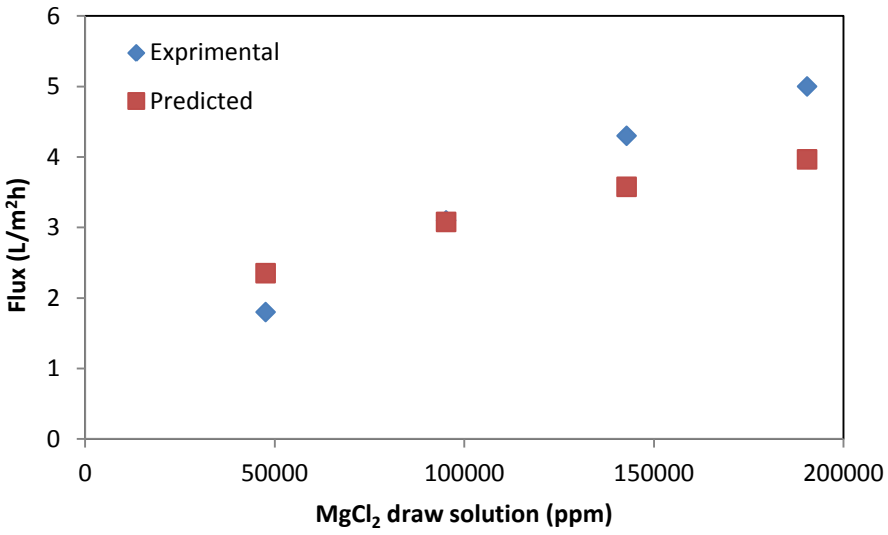

Figure 24: Flux as a function of draw solution concentration, data from J. Su et al. [22]

Figure 24 shows the water flux as a function of the draw solution concentration. The feed solution concentration was constant (deionized water) and the effect of the draw solution concentrations was observed. As shown in Figure 24, the predicted water flux is in a good agreement with the experimental measurement of J. Su et al. [22] with a higher accuracy at lower water flux. The feed solution was assumed to have zero osmotic pressure; therefore, the second part of the flux model was eliminated. In addition, the feed mass transfer coefficient had no impact on the predicted flux. The predicted water flux with dilutive ICP was between 2 to 4 L/m^2h for the given draw solution concentrations. In the contrary, the predicted water flux using the first model that did not take into consideration concentrative ECP and dilutive ICP (Eq. 3, section 1.7.1) was in the range of 18 to120 L/m^2h for the given draw solution concentration. Since concentrative ECP did not influence water flux, the reduction in water flux in this process was solely due to dilutive ICP.

The findings of J. McCutcheon et al. [13] study to examine the effectiveness of the draw solution at different concentrations were also modeled. In their study, they examined the relationship between draw solution concentrations, feed solution concentrations, and water flux. In search of an ideal draw solution, they reported that

ammonia and carbon dioxide mixture had met all required criteria for a draw solution. The selected draw solution generated high osmotic pressure. It was highly soluble in water and may be recovered via an inexpensive separation process.

The experimental setup of J. McCutcheon et al. [13] was a SEPA cell (GE Osmonics, Trevose, PA) with modified channels. Co-current flow of the feed and draw solutions was used in the all runs. The draw solution was prepared by mixing ammonium bicarbonate and ammonium hydroxide with deionized water. The ratio of ammonia to carbon dioxide ranged from 1.2 to 1.4 M for draw solutions of 1.1 to 6 M. The temperature of the feed and draw solutions were maintained at 50±1 ºC by a water bath for the feed solution and a heating mantle for the draw solution. Water flux was determined by measuring the rate of weight change in the draw solution. The membrane was provided by Hydration Technologies Inc. (Albany, OR) with proprietary morphology.

As for the flux modeling parameters, the water permeability coefficient was determined and reported as 5.69×10^{-12} m/Pa·s. The solute permeability coefficient was assumed to be zero because of the low salt leakage. The osmotic pressure of both the feed and draw solutions were determined using the OLI software and were given in the study. The mass transfer coefficient was calculated using the given system dimensions and parameters. Using the above parameters and the steps mentioned earlier (section2.5), the solute resistance to diffusion was calculated. The average value of solute resistance to diffusion was found to be 3.24E5 s/m, which was used for the water flux prediction. The study was conducted for various feed concentrations. See Figure 25 for the results.

Figure 25 shows water flux as a function of draw solution concentration for experimental and predicted flux. A constant NaCl feed solution was used with concentration of 2,922 ppm NaCl. The highest water flux was exhibited at draw solution concentration of 6 M due to highest driving force available. The feed solution was gradually increased as shown in Figure 26.

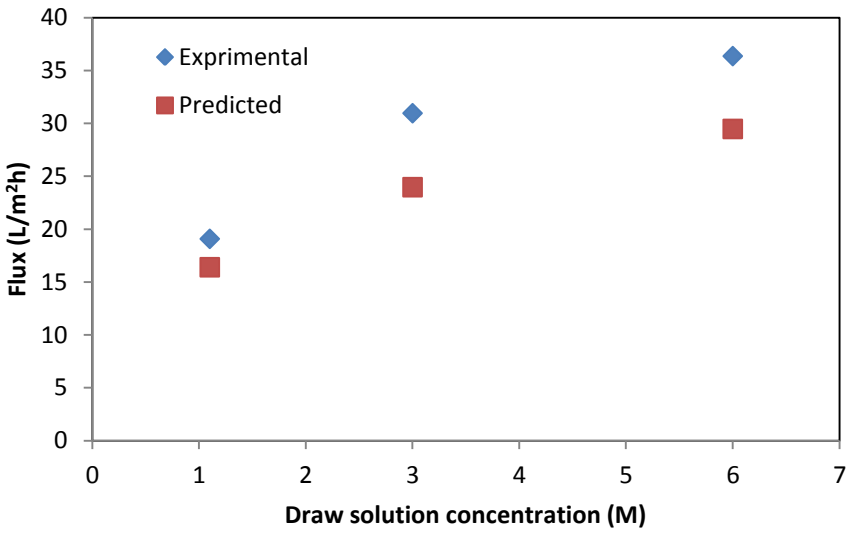

Figure 25: Flux as a function of draw solution concentration for NaCl feed solution of 2922 ppm

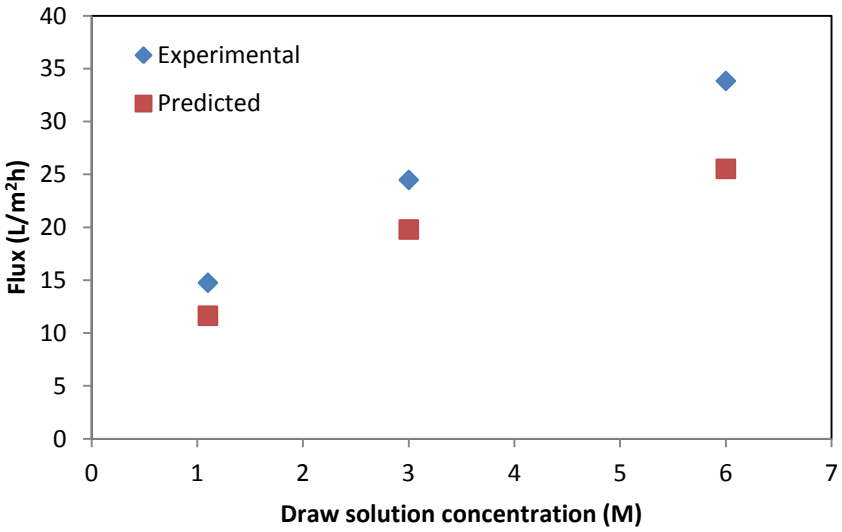

Figure 26: flux as a function of draw solution concentration for NaCl feed solution of 11680 ppm

Figure 26 shows water flux as a function of draw solution concentration where a constant NaCl feed solution was used with concentration of 11,680 ppm NaCl. It was observed that as the feed concentration was increased; the water flux was reduced due to the lower osmotic pressure difference.

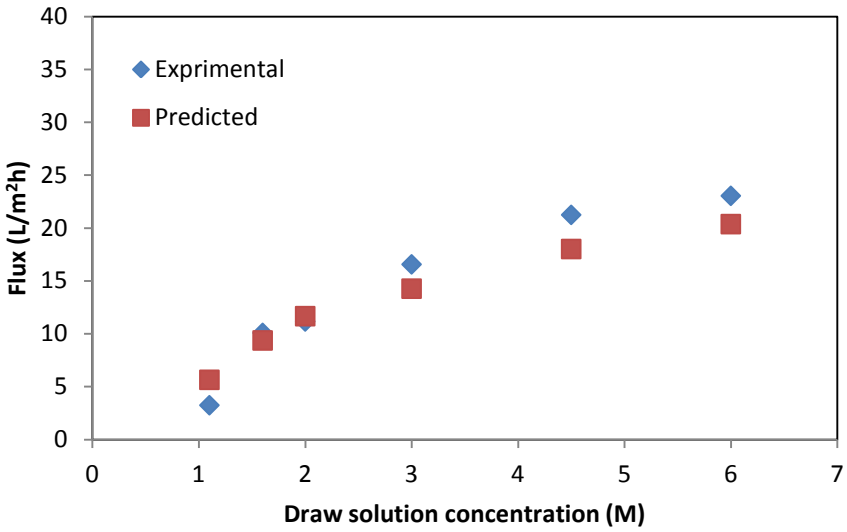

Figure 27: Flux as a function of draw solution concentration for NaCl feed solution of 29220 ppm

Figure 27 shows water flux as a function of draw solution concentration where a constant NaCl feed solution was used with concentration of 29,220 ppm NaCl. In general, because the feed concentration was increased; lower flux was exhibited due to lower driving force. From the experimental data it was seen that when the feed solution concentration was increased by a factor of 2.5, overall water flux decreased by 10L/m^2h.

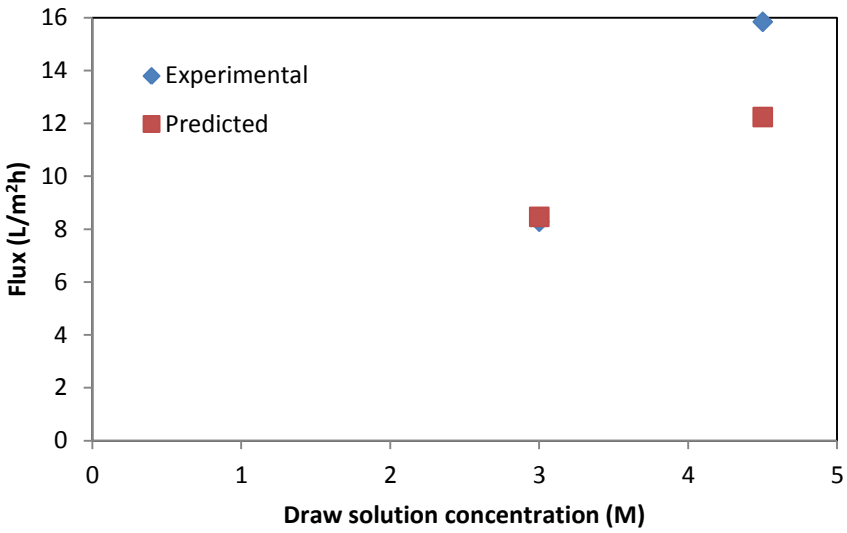

Figure 28: Flux as a function of draw solution concentration for NaCl feed solution of 58440 ppm

The feed solution concentration was further increased and flux was predicted. Figure 28 shows water flux as a function of draw solution concentration where a constant NaCl feed solution was used with concentration of 58,440 ppm NaCl. From the figure it was observed that at lower water flux, the model had a better fit to experimental data.

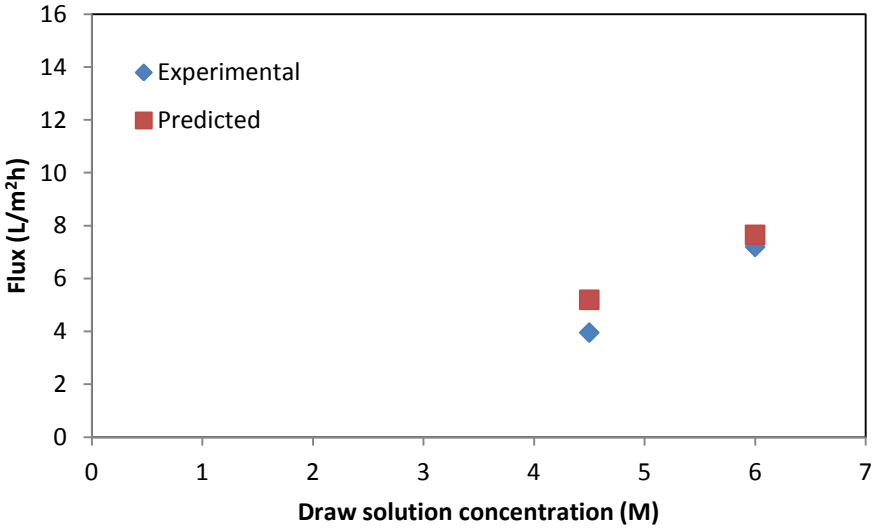

Figure 29: Flux as a function of draw solution concentration for NaCl feed of 116880 ppm

Figure 29 shows water flux as a function of draw solution concentration where a constant NaCl feed solution was used with concentration of 116,880 ppm NaCl. Overall, with various feed and draw solution concentrations the flux model prediction was a good fit to the experimental data. Similar to previous cases, the model prediction was more accurate for lower water flux. The difference between the predicted and experimental flux at 2,922 ppm feed solution was 5 L/m^2h, while the difference at 116,880 ppm feed solution was less than 0.4 L/m^2h. It was also observed, as the feed concentration was increased, the flux reduced and the flux prediction became more accurate. Figure 27 clearly shows a property of Eq.13, in which increasing the draw solution concentration infinitely, therefore the driving force, did not increase the flux. The model had a good flux prediction at different system conditions. Using the model in such a study would have reduced the experimental work associate to study and optimize the system.

Further the flux model was tested using the study of McCutcheon [17]. In the study, the flux was examined for both forward osmosis process and pressure retarded osmosis process. The effects of ECP and ICP were examined, in addition, to the effect of temperature on flux. The experimental setup was a SEPA cell (GE Osmonics, Trevose, PA) with modified channels on both sides of the membrane. The feed and the draw solutions were pumped in channels normal to the membrane flux. Temperatures of both solutions were regulated using a water bath. Water flux was measured by the change in weight of the draw solution. The feed and draw solutions were NaCl solutions in which, draw solution concentration was constant and the feed solution concentration was varied. See Figure 30 for results.

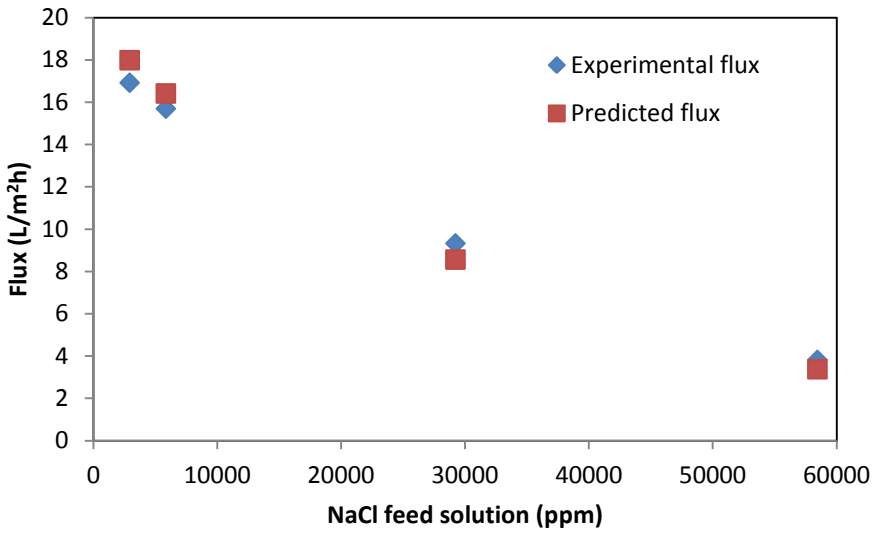

Figure 30: Flux as a function of feed solution concentration, experimental and predicted flux data from J. McCutcheon [17]

Figure 30 shows the predicted and measured water flux as a function of feed solution concentration. The model had a very good fit to the experimental results. The Figure also verifies the accuracy of the flux model. Comparing our experimental measurements to J. McCutcheon [17], our flux was much lower which might be due to experimental setup differences. Our process was based on molecular defuse and natural osmosis, while J. McCutcheon [17] had a pump for feed and draw solution circulation. Also the solute resistance to diffusion, *K*, of both membranes were calculated and found to be 1.6E06 s/m for our membrane and 2.5E05 s/m for J. McCutcheon's [17] membrane. It indicates that the membranes have different properties which results in different value flux.

Flux modeling was also performed on the findings of C.H. Tan and H.Y. Ng [30]. In their study, C.H. Tan and H.Y. Ng. performed many experimental trials in efforts to improve the prediction of solute resistance to diffusion. They developed a model to predict the solute resistance to diffusion which was independent of solute diffusion coefficient. In previous calculations performed in this study, the average solute resistance to diffusion was used for flux prediction. This assumption was explained by a constant

diffusion coefficient regardless of the changes in concentration, which may be seen in Eq.7. The model for solute resistance to diffusion was a function of flux, bulk draw solution concentration, and draw solution concentration at the membrane wall. The model was developed from a differential equation with diffusion coefficient embedded within. Hence, a diffusion coefficient correlation was developed for NaCl. The modified solute resistance to diffusion model developed by C.H. Tan and H.Y. Ng. [30] was only applicable to systems where the draw solution was NaCl solution.

The membrane cell used in their study was specially designed a cross-flow membrane cell with the required dimensions. The feed and draw solution were circulated in a co-current manner and maintained at 30ºC. The water flux was determined by monitoring the weight changes in the draw solution. The membrane was provided by Hydration Technologies Inc. (Albany, OR). It was a cellulose acetate asymmetric membrane. For the data used, the membrane orientation was as follows, the feed solution was against the active membrane surface and the draw solution was against the porous support layer. The feed solution was deionized water, assumed to be free of salts; therefore, had zero osmotic pressure. Deionized water was used as a feed solution to eliminate the concentrative ECP phenomenon and to examine the dilutive ICP independently. The draw solution was NaCl solution with various concentrations, while the feed solution had constant concentration. At the given draw solution concentrations, the runs were conducted at three different flow rates to ensure that flow rate had a negligible impact on water flux.

The solute resistance to diffusion was calculated, using Eq. 11, as the average of three different draw solution cross flow rates. The average solute resistance to diffusion was found to be 1.83E05 s/m. The water permeability coefficient was determined experimentally by C.H. Tan and H.Y. Ng [30] and found to be 4.00E-07 m/atm·s. The feed mass transfer coefficient had no impact on the flux prediction since feed osmotic pressure was assumed to be zero. Salt permeability coefficient, *B*, was assumed to be zero. See Figure 31 for modeling results.

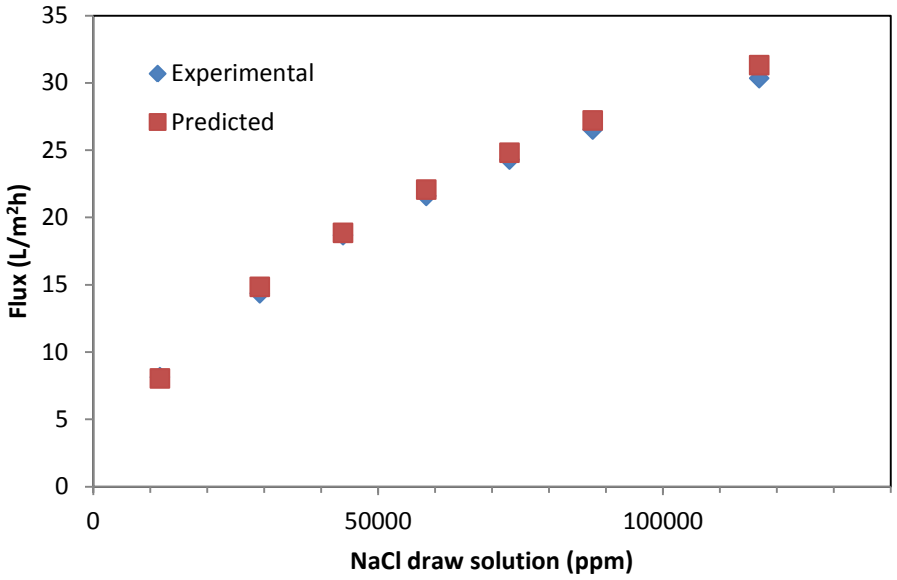

Figure 31: Flux as a function of draw solution concentration from C.H. Tan and H.Y. Ng [30]

Figure 31 shows water flux as a function of NaCl draw solution concentration. The experimental results of C.H. Tan and H.Y. Ng [30] showed identical water flux at different draw solution flow rate. Therefore, the flux in Figure 31 was only for draw solution flow rate of 1 L/min. The model accurately predicted the same conclusion that the flux was independent of the draw solution flow rate since the flux model was not a function of draw solution flow rate (see Appendix A). The model prediction was in agreement with the experimental data available with high accuracy at both high and low water flux.

3.4. Forward Osmosis Analysis with Magnesium Sulfate as Draw Solution

The first system to be analyzed was the sea water and brackish water feed solutions with magnesium sulfate draw solutions. Under the experimental conditions described earlier, each run was repeated twice for each feed solution and the average flux was found. See Table 3 and 4 for the results.

Table 3: Flux experimental results for seawater feed and magnesium sulfate draw solution

Start time (min)	End time (min)	Change in volume ΔV (ml)	Flux (L/m^2h)
0	135	1.25	0.9
0	1090	6.25	0.56
		Average flux	0.6

Table 4: Flux experimental results for brackish water feed and magnesium sulfate draw solution

Start time (min)	End time (min)	Change in volume ΔV (ml)	Flux (L/m^2h)
0	30	1.25	4.06
0	30	1.25	4.06
		Average flux	4.06

3.4.1 Flux modeling with magnesium sulfate as draw solution. Two experimental runs were done with magnesium sulfate as a draw solution. The draw solution concentration was 240,000 ppm which was below the saturation point. One run was for a feed solution of 5,000 ppm NaCl solution to represent brackish water and the other was a feed of 40,000 ppm to represent sea water. The change in volume was observed with time to determine the flux. Flux was determined using Eq.13 and compared with the experimental flux, the comparison results are shown in Figures 32 and 33.

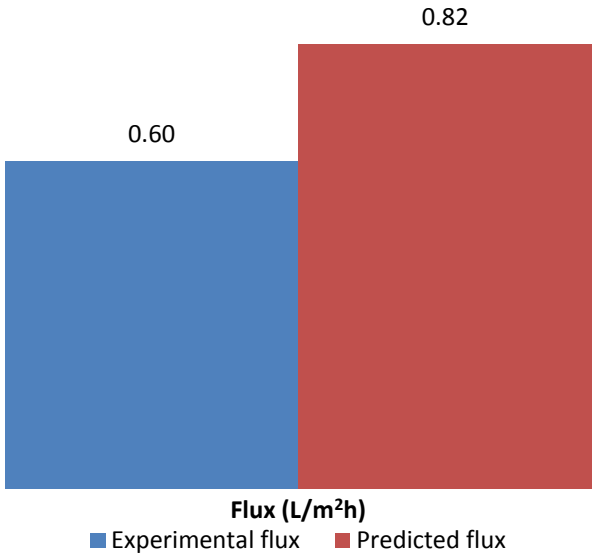

Figure 32 : Flux comparison with sea water feed and magnesium sulfate draw solution

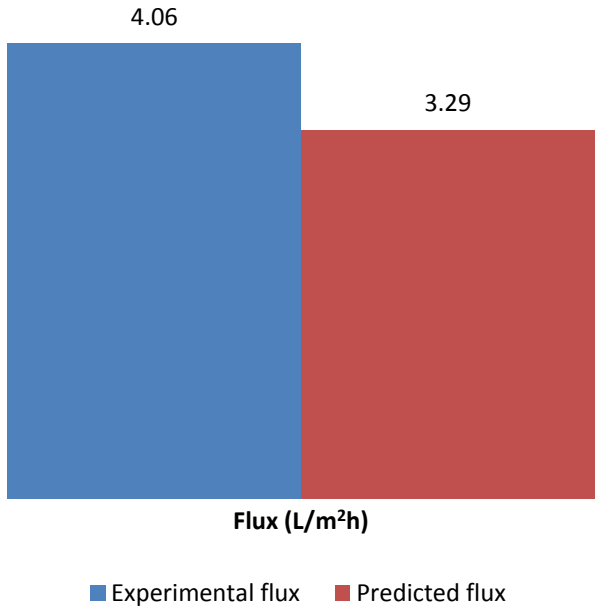

Figure 33: Flux comparison with brackish water feed and magnesium sulfate draw solution

The model had a good approximation of flux in the FO process. The error in flux prediction was maybe due the assumption of constant diffusion coefficient. It might be

also attributed to the use of the average solute resistance to diffusion *K*, determined from the experimental flux, in the flux modeling.

To understand the source of low flux exhibited in the experiment, the osmotic driving force was calculated and it is shown in Table 5.

Table 5: Apparent and effective driving force for brackish and sea water feed and magnesium sulfate as draw solution

Feed type	Apparent driving force ($\pi_{D,b}$- $\pi_{F,b}$) (kPa)	Effective driving force ($\pi_{D,i}$- $\pi_{F,m}$) (kPa)
Sea water	2,317.4	70.57
Brackish water	5,137.5	400.8

The driving force for sea water feed was reduced from 2310 kPa to 70 kPa. While the driving force was reduced from 5140 kPa to 400 kPa for brackish water feed solution.

3.4.2 Concentrative ECP for magnesium sulfate as draw solution. To further understand the influence of concentrative ICP on flux, the bulk and membrane osmotic pressures were examined. The osmotic pressure of the bulk feed solution for brackish and sea water were 396.5 and 3,217.6 kPa respectively. On the other hand, feed membrane surface osmotic pressure that was determined by Eq.1 was 423.1 and 3,248.6 kPa for brackish and sea water respectively. It can be observed that the increase of feed osmotic pressure was very low, therefore did not influence flux reduction drastically. High concentrative ECP can easily be reduced by increasing feed velocity and turbulence.

3.4.3 Dilutive ICP for magnesium sulfate as draw solution. As for the draw solution osmotic pressure, the bulk osmotic pressure for 240,000 ppm $MgSO_4$ solution was 5,534 kPa. The draw solution osmotic pressure within the support layer was

calculated using Eq.12. It was found to be 832.9 kPa, when the feed was brackish water, and 3,319 kPa when the feed was sea water. The concentration of the draw solution within the support layer was lower than the bulk concentration therefore the osmotic pressure was lower. It can be seen that dilutive ICP had a major impact on draw solution osmotic pressure and the reason of the reduction of osmotic pressure driving force. The dilutive ICP had a higher impact on draw solution osmotic pressure when the feed was brackish water, which occurred because brackish feed water flux was higher leading to a lower draw solution concentration within the support layer compared to sea water feed. It was also understood more from Figure 34, which shows the ratio of osmotic pressure within the support layer to draw solution bulk osmotic pressure (π_{Di}/π_{Db}) as a function feed concentration.

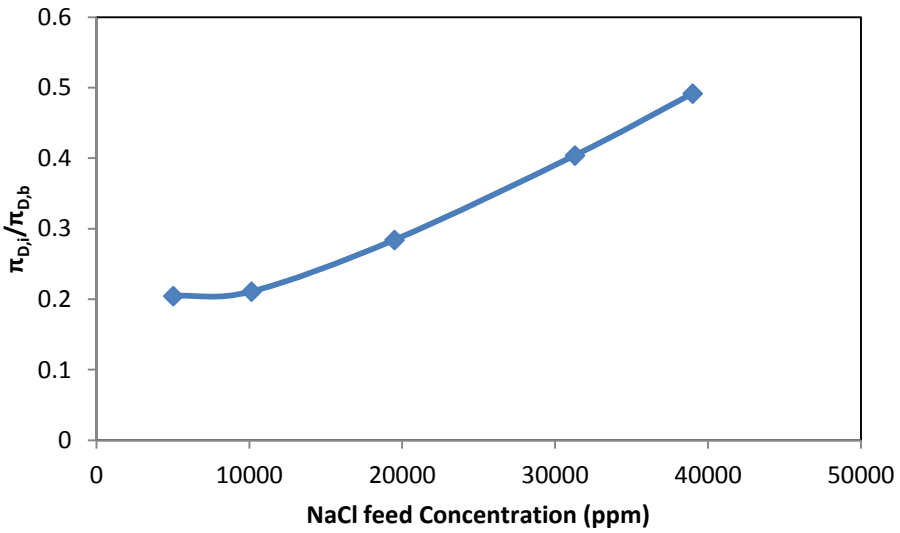

Figure 34: Effect of feed water concentration on membrane support to bulk osmotic pressure ratio- NaCl draw solution

It was noticed that as the feed concentration increased so did the membrane support layer to bulk osmotic pressure ratio due to the reduced flux. The closer π_{Di}/π_{Db}

was to one, the closer osmotic pressure inside the active layer within the membrane porous support was to bulk osmotic pressure reducing dilutive ICP.

3.4.4 Effect of feed mass transfer coefficient (*k*) on flux and ECP with $MgSO_4$ draw solution. Another factor that affects flux in an FO process with dilative ICP and concentrative ECP is feed solution mass transfer coefficient. Mass transfer coefficient affects the magnitude of concentrative ECP in the process. Any change in the mass transfer coefficient results in a change of feed solution membrane osmotic pressure. It can be seen that a change in feed osmotic pressure results in a change of overall driving force. Figure 35 shows the effect of mass transfer coefficient on flux.

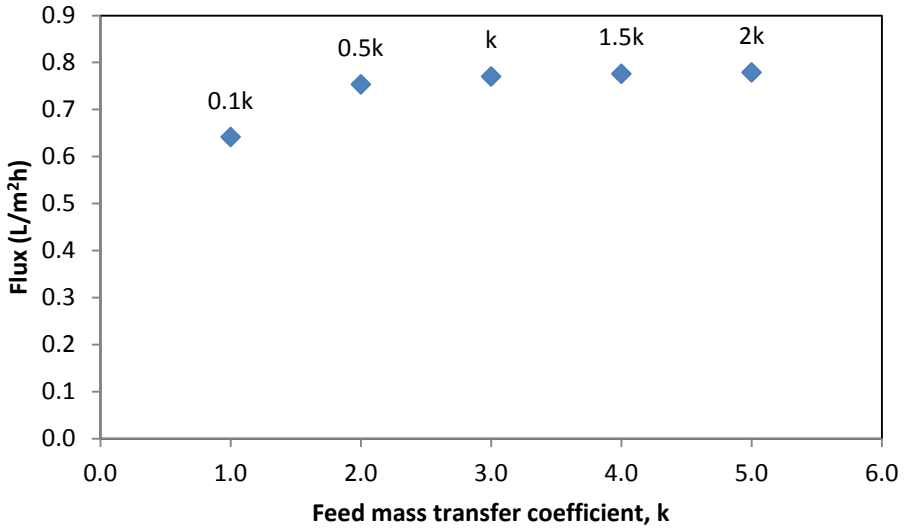

Figure 35: Flux as a function of feed mass transfer coefficient variation with sea water feed solution and magnesium sulfate draw solution

In Figure 35, each point indicates a change in feed mass transfer coefficient by a certain factor. It can be seen that the increase in mass transfer coefficient increases flux in a forward osmosis process. The feed solution for this calculation was sea water.

Figure 36 shows the effect of mass transfer coefficient on the feed membrane surface to bulk osmotic pressure. Mass transfer coefficient was changed by factors of 0.1, 0.5, 1, 1.5, and 2.

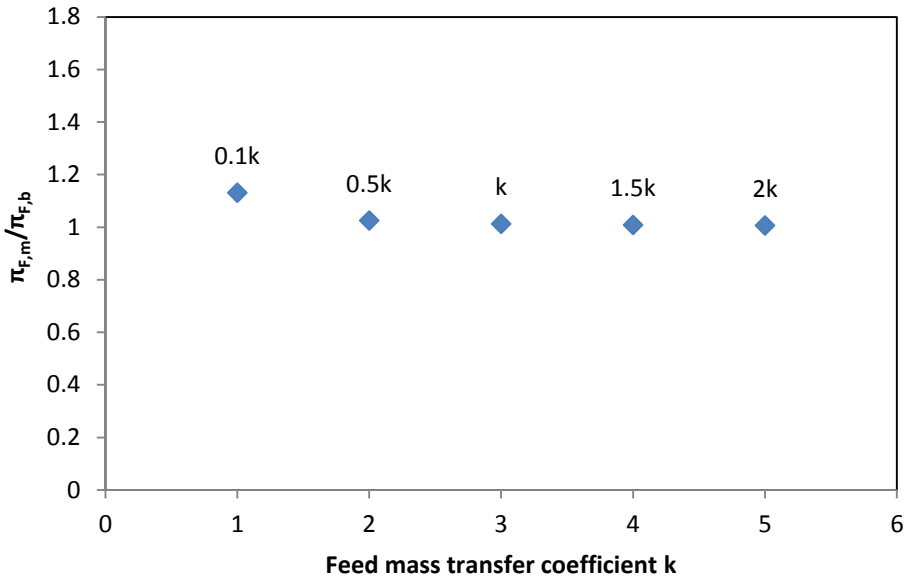

Figure 36: Feed membrane surface osmotic pressure to bulk osmotic pressure, $\pi_{F,m}/\pi_{F,b}$, as a function of mass transfer for sea water feed and magnesium sulfate draw solution

It can be observed from Figure 36 that as the feed mass transfer coefficient increases, the membrane active layer osmotic pressure becomes closer to the feed bulk osmotic pressure. Higher feed mass transfer coefficient leads to a reduction in concentrative ECP.

As for the effect of mass transfer coefficient on flux for brackish water feed, the only difference occurs from the flux. The flux increase due to mass transfer increase was significant, which can be seen from Figure 37. As for the effect on concentrative ECP, high concentrative ECP was observed at one tenth the mass transfer coefficient. As for the remaining values of mass transfer coefficient, concentrative ECP was observed to be at a minimum.

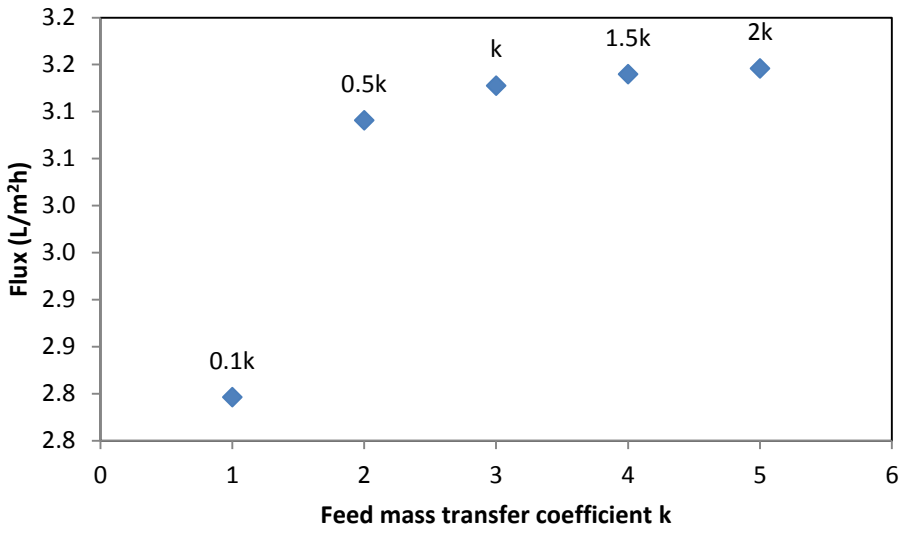

Figure 37: Flux as a function of feed mass transfer coefficient variation with brackish water feed solution and magnesium sulfate draw solution

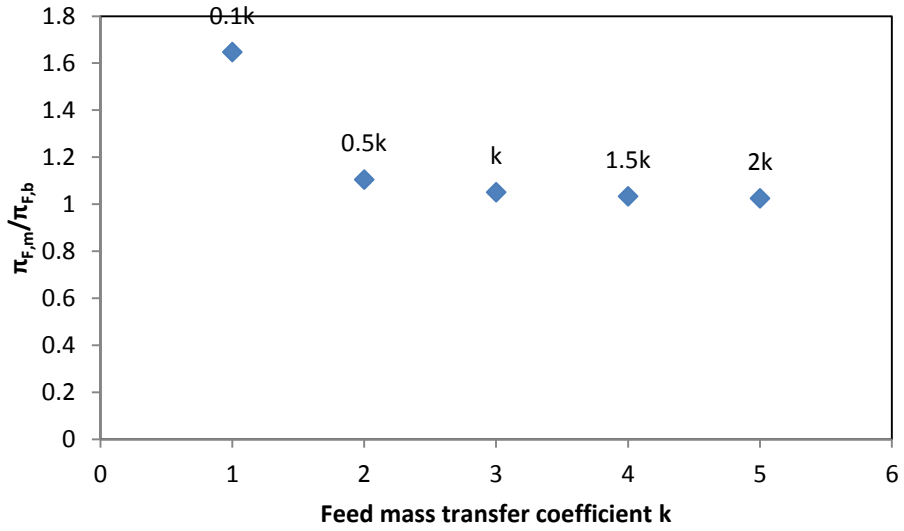

Figure 38: Feed membrane surface osmotic pressure to bulk osmotic pressure, $\pi_{F,m}/\pi_{F,b}$, as a function of feed mass transfer for brackish water feed and magnesium sulfate draw solution

From Figure 38, it was clear that, although mass transfer coefficient affected the flux and concentrative ECP in a forward osmosis process, the increase in flux and reduction in concentrative ECP was minor. The slight increase in flux can attributed to the reduction in concentrative ECP in the membrane. Since concentrative ECP was minor in the conducted experiment, an increase in the feed mass transfer coefficient resulted in a small change in concentrative ECP.

3.5. Forward Osmosis Analysis with Copper Sulfate as Draw Solution

3.5.1 Flux modeling with copper sulfate as draw solution. Similar runs to magnesium sulfate runs were carried out for copper sulfate draw solution. Copper sulfate had a lower solubility limit, therefore lower flux was expected. The selected draw solution was copper sulfate with 200,000 ppm concentration. Initially brackish and sea water were proposed for the experimental trial, but sea water osmotic pressure was found to be higher than the draw solution osmotic pressure therefore the forward osmosis process was not feasible.

Brackish water and copper sulfate draw solution run was conducted twice and the average flux was determined. Figure 39 shows the result and comparison of the experimental and predicted flux. The model had a good flux prediction.

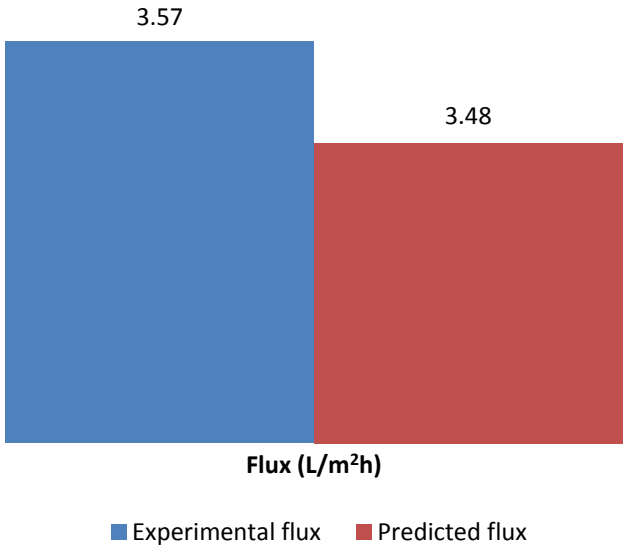

Figure 39: Experimental and predicted flux comparison for brackish water feed and copper sulfate draw solution

For copper sulfate modeling also, the average *K* introduced slight error. The experimental flux was higher than the predicted flux due to the fact that the average *K* was higher than the *K* that was determined from experimental data. Experimental flux was found to be lower than the calculated flux (assuming no ECP and ICP), which exposed the significant effects of ECP and ICP on flux. The great reduction in flux was mainly due to the reduction of the osmotic driving force. Table 6 displays the drop in driving force.

Table 6: Apparent and effective driving force for brackish water feed and copper sulfate draw solution

Feed type	Apparent driving force ($\pi_{D,b}$- $\pi_{F,b}$) (kPa)	Effective driving force ($\pi_{D,i}$- $\pi_{F,m}$) (kPa)
Brackish water	2303.5	351.0

3.5.2 Concentrative ECP for copper sulfate as draw solution. Although concentrative ECP had no major impact on the FO process flux, the increase in feed solution osmotic pressure had to be determined to ensure it was at minimum. The bulk feed solution osmotic pressure was 396.5 kPa, while the active layer membrane surface osmotic pressure was found to be 419.8 kPa. The slight increase in osmotic pressure did not count for the large drop in osmotic driving force.

3.5.3 Dilutive ICP for copper sulfate as draw solution. To identify the effect of dilutive ICP, the draw solution osmotic pressure within the membrane support layer had to be found. The draw solution bulk osmotic pressure was 2,700 kPa, and the osmotic pressure within the membrane support layer was 770.8 kPa. From this information, it was concluded that dilutive ICP was the major contributor to flux reduction in FO process.

3.5.4 Effect of feed mass transfer coefficient (*k*) on flux and ECP with $CuSO_4$ draw solution. The effect of feed mass transfer coefficient on the flux with brackish feed and copper sulfate draw solution was also examined. The flux was almost constant when the mass transfer coefficient was doubled. Figure 40 confirmed that increasing mass transfer coefficient was of small effect on flux.

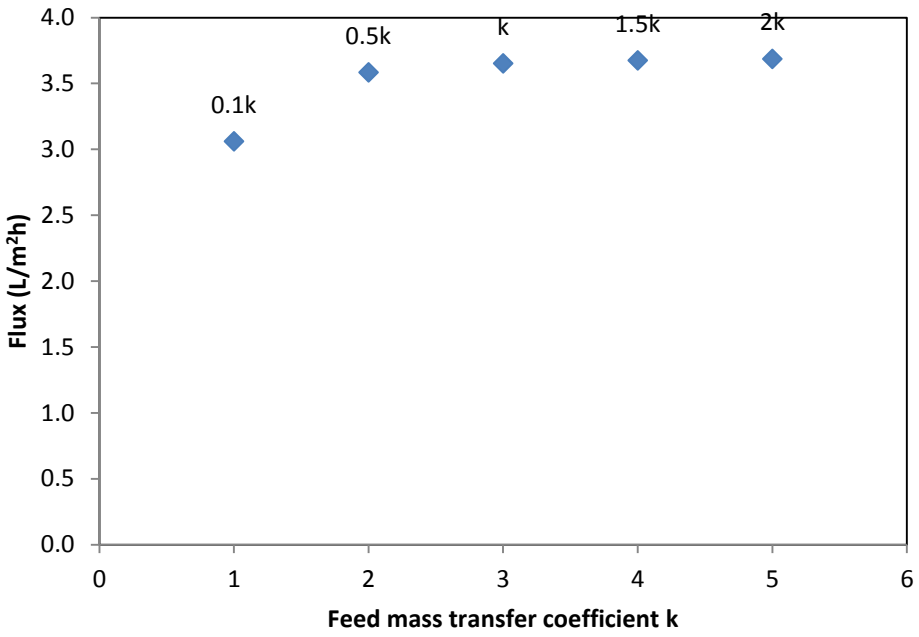

Figure 40: Flux as a function of feed mass transfer coefficient variation with copper sulfate draw solution

Moreover, the effect of the mass transfer coefficient on concentrative ECP is shown in Figure 41. Primarily, it was observed that at experimental conditions concentrative ECP was very low and bulk and membrane surface feed osmotic pressures were almost identical. An increase in the mass transfer coefficient brought membrane surface osmotic pressure closer to bulk osmotic pressure, but with no major significance.

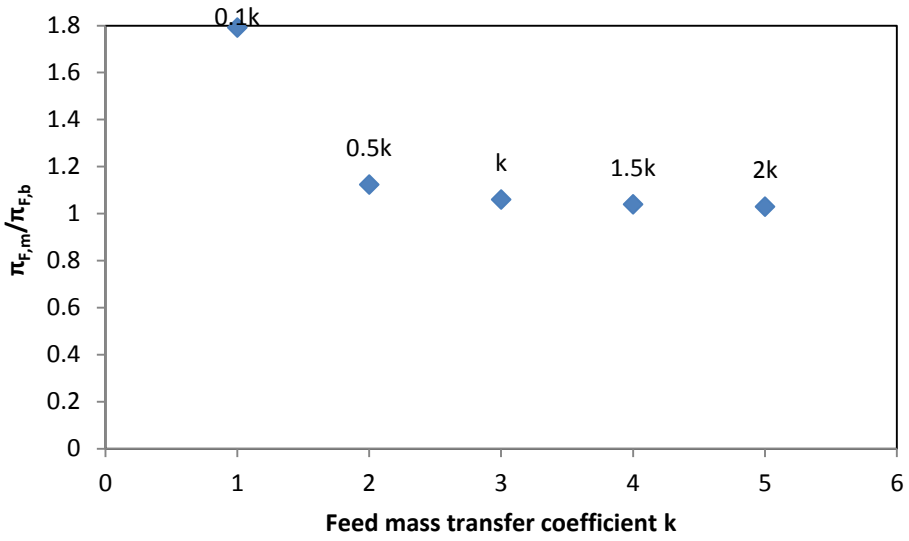

Figure 41: Feed membrane surface osmotic pressure to bulk osmotic pressure, $\pi_{F,m}/\pi_{F,b}$, as a function of feed mass transfer for copper sulfate draw solution

3.6. Magnesium and Copper Sulfate Flux Comparison

To compare the performance of magnesium and copper sulfate draw solutions in terms of water flux, osmotic pressure of the two solutions had to be equal. Since copper sulfate had a lower solubility limit, the selected osmotic pressure for both draw solutions can be used for brackish water FO. Throughout the flux calculation the mass transfer coefficient, feed osmotic pressure and draw solution osmotic pressure were the same for both draw solutions. The difference between the draw solutions when determining the flux was the solute resistance to diffusion. Although identical membranes were used, the difference in solute resistance to diffusion occurred due to the difference in diffusion coefficient. The result of flux modeling is shown in Figure 42.

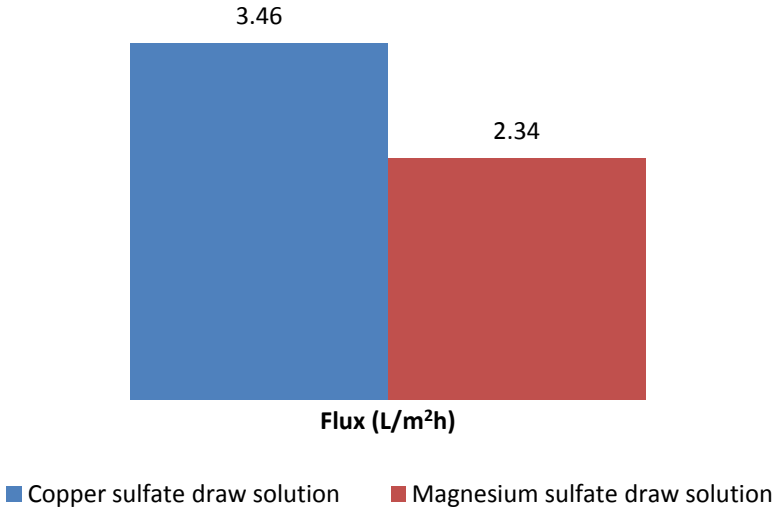

Figure 42: Flux comparison between copper sulfate and magnesium sulfate draw solutions

The determined flux was based on theoretical calculation since the selected model had been proven to be applicable to systems of copper sulfate and magnesium sulfate draw solutions. At an osmotic pressure of 26.7 atm, it was determined that copper sulfate draw solution produced higher water flux compared to magnesium sulfate at the same osmotic pressure. The water flux was higher for copper sulfate draw solution due to the lower solute resistance to diffusion with a value of 1.35E06 s/m, while magnesium sulfate had a solute resistance to diffusion of 2.24E06 s/m.

3.7. Effect of Solute Resistance to Diffusion (*K*) on Dilutive ICP

Dilutive ICP occurs due to the dilution of draw solution within the membrane support layer. Therefore, to reduce the effect of dilutive ICP the membrane support layer has to be altered. In the ICP and ECP flux model, *K*, solute resistance to flow is the source of reduction in flux. *K* is a function of draw solution diffusion coefficient, membrane thickness, tortuosity and porosity. The properties of the membrane that was used in all experiments were HTI proprietary. Keeping the same draw solution, when *K* is varied, the remaining factors; membrane thickness, tortuosity, and porosity are changing.

K is directly proportional to membrane thickness, tortuosity and inversely proportional to porosity and solute diffusion coefficient. To determine its effect, *K* was varied with reference to the calculated *K*. The effect of changes in *K* on π_{Di}/π_{Db} is shown in Figure 43.

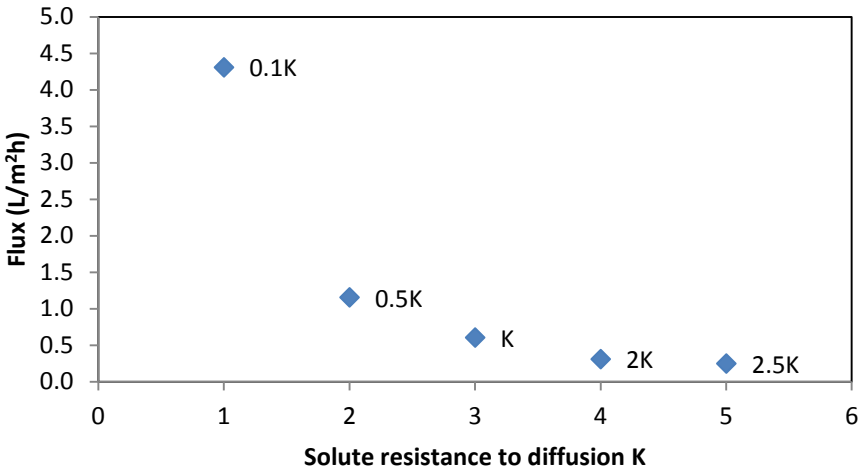

Figure 43: Flux as a function of solute resistance to diffusion

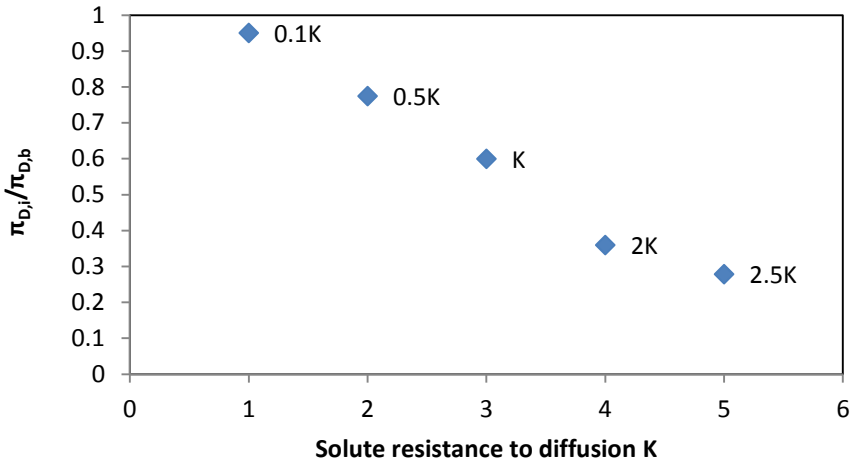

Figure 44: Osmotic pressure within the membrane support layer to bulk draw solution osmotic pressure ratio, π_{Di}/π_{Db} as a function on solute resistance to diffusion

Figure 43 shows the flux as a function of solute resistance to diffusion. It was observed that increasing the solute resistance to diffusion led to a reduction in flux. Thus,

when designing a FO membrane, low solute resistance to diffusion is favorable to obtain high flux.

For all cases, magnesium and copper sulfate draw solutions, π_{Di}/π_{Db} ratio was inversely proportional to the solute resistance to diffusion. As the draw solution resistance to diffusion in the membrane support layer increased above a value based on experimental data, the dilutive ICP effect increased. Figure 44 shows as the *K* value decreased below the experimental calculated value, the dilutive ICP effect decreased. Figure 44 may also show that an increase in thickness or tortuosity cause an increase in dilutive ICP effect. On the other hand, if the membrane porosity was increased; dilutive ICP effects would be lower.

Chapter 4: Conclusion

With increasing water demand, FO desalination became a great candidate as an alternative to generate water with superior benefits compared to other desalination processes. The objective of this study was to calculate the water flux, determine factors affecting the flux, and determine ways to improve forward osmosis membranes. The proposed flux model was tested with our experimental data and data from the literature. The model was in agreement with most obtained data. Flux modeling with two draw solutions, magnesium sulfate and copper sulfate, was also performed. The experimental flux was found to be in agreement with the predicted flux when the effects of concentrative ECP and dilutive ICP were included in the model. The dilutive ICP was found to be the major contributor to flux reduction, while the effect of the concentrative ECP on the effective driving force was minor. Other factors that influenced the flux in forward osmosis where also studied in an attempt to improve the process.

The effect of solute resistance to diffusion (K) on the flux and on the ratio of draw solution osmotic pressure within the membrane support layer to bulk osmotic pressure was also studied. It was found that as the solute resistance to diffusion was decreased, the draw solution osmotic pressure within the membrane support layer approached the bulk draw solution osmotic pressure. To reduce dilutive ICP effects, K has to be reduced as much as possible. Small K values may be achieved by a thinner membrane layer and a more porous membrane support keeping in mind high selectivity. Also less dilutive ICP was exhibited using a higher feed concentration which was due to the lower flux.

Comparing both draw solutions with brackish water feed solution, copper sulfate exhibited less dilutive ICP, which was due to larger molecular weight. Also copper sulfate draw solution resulted in a higher predicted flux compared to magnesium sulfate. Magnesium sulfate has the benefit of having higher osmotic pressure than copper sulfate. On the other hand, magnesium sulfate is not recommended as a draw solution because of its higher scaling potential.

As for the effect of mass transfer coefficient on concentrative ECP, it was reported in the literature that an increase in the feed mass transfer coefficient would

reduce concentrative ECP effects, which was confirmed by this study. In our work, an increase in mass transfer coefficient had a small effect on flux and concentrative ECP since the increase in feed osmotic pressure at the membrane surface was small.

The Optimization of the forward osmosis process is very important to make the process commercially available at a low production cost. Further research is needed to determine the optimum solute to resistance to diffusion ratio. Also there is a need to determine the best draw solution concentration relative to the feed solution because it will impact the draw solution regeneration costs.

Appendix A

Calculation results

1. Data from G. Gray et al. [29]

Feed solution concentration (M)	Feed solution osmotic pressure (atm)	Draw solution concentration (M)	Draw solution osmotic pressure (atm)	K(day/m)	Experimental flux (L/m^2h)	Predicted flux (L/m^2h)
0.0625	2.88	0.5	22.43	4.091	7.7083	8.84
0.122	5.58	0.5	22.43	3.458	6.875	7.23
0.249	11.08	0.5	22.43	3.003	4.5416	4.43
0.375	16.7	0.5	22.43	2.580	2.2916	2.05

Average solute resistance to diffusion, K (s/m)	2.84E+05
Water permeability coefficient, A (m/atm·day)	0.027
Solute permeability coefficient, B (m/day)	0.021
Mass transfer coefficient, k (m/s)	1.74E-05

2. Data from J. Su et al. [22]

Draw solution concentration (M)	Draw solution concentration $MgCl_2$ (ppm)	Draw solution osmotic pressure (atm)	Feed solution osmotic pressure (atm)	K (m^2h/L)	Experimental flux (L/m^2h)	Predicted flux (L/m^2h)
0.5	47605	38.10	0	1.283579	1.8	2.35
1	95210	91.99	0	0.854298	3.1	3.08
1.5	142815	164.24	0	0.674595	4.3	3.58
2	190420	254.94	0	0.637932	5	3.97

Average solute resistance to diffusion, K (s/m)	3.11E+06
Water permeability coefficient, A ($L/m^2bar{\cdot}h$)	0.47

3. Data from J. McCutcheon [13]

Feed solution concentration (M)	Feed solution osmotic pressure (atm)	Draw solution concentration (M)	Draw solution osmotic pressure (atm)	K (s/m)	Experimental flux (L/m^2h)	Predicted flux (L/m^2h)
0.05	2.5	1.1	47.4	2.64E+05	19.08	16.40
0.05	2.5	3	127.6	2.31E+05	30.96	23.96
0.05	2.5	6	249.5	2.49E+05	36.36	29.47
0.2	9.8	1.1	47.4	2.51E+05	14.76	11.64
0.2	9.8	3	127.6	2.61E+05	24.48	19.79
0.2	9.8	6	249.5	2.40E+05	33.84	25.53
0.5	24.8	1.1	47.4	6.49E+05	3.24	5.64
0.5	24.8	1.6	73.3	3.22E+05	10.08	9.36
0.5	24.8	2	94.5	3.67E+05	11.16	11.66
0.5	24.8	3	127.6	2.95E+05	16.56	14.26

0.5	24.8	4.5	193.3	2.89E+05	21.24	18.01
0.5	24.8	6	249.5	3.02E+05	23.04	20.37
1	51.5	3	127.6	3.61E+05	8.28	8.46
1	51.5	4.5	193.3	2.69E+05	15.84	12.24
2	113.8	4.5	193.3	4.64E+05	3.96	5.20
2	113.8	6	249.5	3.76E+05	7.20	7.66

Average solute resistance to diffusion, K (s/m)	3.24E+05
Water permeability coefficient, A ($L/m^2bar \cdot h$)	5.69E-12
Mass transfer coefficient, k (m/s)	6.31E-05

4. Data from J. McCutcheon [17].

Feed solution concentration (M)	Feed osmotic pressure (atm)	Draw solution osmotic pressure (atm)	K s/m	Experimental flux (L/m^2h)	Predicted flux (L/m^2h)
0	0	70.04	2.87E+05	18.18	19.84
0.05	3.06	70.04	2.74E+05	16.92	17.99
0.1	6	70.04	2.66E+05	15.70	16.41
0.5	27.11	70.04	2.17E+05	9.32	8.56
1	49.63	70.04	2.07E+05	3.82	3.38

Average solute resistance to diffusion, K (s/m)	2.50E+05
Water permeability coefficient, A (m/atm·s)	3.13E-07
Mass transfer coefficient, k (m/s)	1.74E-05

5. Data from C.H. Tan & H.Y. Ng [30].

Draw solution flow rate	Feed osmotic pressure	Draw solution concentration (M)	Draw solution osmotic pressure (atm)	K(s/m)	Experimental flux (L/m^2h)	Predicted flux (L/m^2h)
1L/min	0	0.2	8.4	1.75E+05	8.14	8.04
	0	0.5	21.9	1.97E+05	14.36	14.85
	0	0.75	34.1	1.86E+05	18.68	18.86
	0	1	47	1.90E+05	21.60	22.07
	0	1.25	60.7	1.90E+05	24.30	24.81
	0	1.5	75.2	1.91E+05	26.53	27.21
	0	2	106.6	1.92E+05	30.35	31.32
2L/min	0	0.2	8.4	1.40E+05	8.64	8.04
	0	0.5	21.9	1.94E+05	14.47	14.85
	0	0.75	34.1	1.91E+05	18.47	18.86

	0	1	47	1.84E+05	22.00	22.07
	0	1.25	60.7	1.80E+05	25.02	24.81
	0	1.5	75.2	1.96E+05	26.14	27.21
	0	2	106.6	1.85E+05	31.03	31.32
3L/min	0	0.2	8.4	1.20E+05	8.96	8.04
	0	0.5	21.9	1.89E+05	14.62	14.85
	0	0.75	34.1	1.91E+05	18.47	18.86
	0	1	47	1.79E+05	22.32	22.07
	0	1.25	60.7	1.84E+05	24.70	24.81
	0	1.5	75.2	1.94E+05	26.32	27.21
	0	2	106.6	1.88E+05	30.74	31.32

Average solute resistance to diffusion, K (s/m)	1.83E+05
Water permeability coefficient, A (L/m^2bar·h)	4.00E-07

6. Initial NaCl trial

Feed solution concentration (ppm)	Feed solution osmotic pressure (atm)	Draw solution concentration (ppm)	Draw solution osmotic pressure (atm)	K (s/m)	Idea flux (L/m^2h)	Experimental flux (L/m^2h)	Predicted flux (L/m^2h)
5030	3.8144574	80000	65.738	5.86E+05	69.665	9.744	4.65
10150	7.83123401	80000	65.738	1.00E+06	65.146	5.594	3.85
19500	15.188745	80000	65.738	1.61E+06	56.868	2.806	2.85
31300	24.544775	80000	65.738	2.38E+06	46.343	1.369	1.98
39000	30.6735668	80000	65.738	2.45E+06	39.448	1.042	1.55

Average solute resistance to diffusion, K (s/m)	1.61E+06
Water permeability coefficient, A (m/atm·s)	3.13E-07
Mass transfer coefficient, k (m/s)	1.74E-05

7. Magnesium sulfate Flux

Feed solution concentration (ppm)	Feed solution osmotic pressure (atm)	Draw solution concentration (ppm)	Draw solution osmotic pressure (atm)	K (s/m)	Experimetnal flux (L/m^{2}h)	Predicted flux (L/m^{2}h)
5000	3.914	240000	54.615	1.69E+06	4.06	3.29
40000	31.754	240000	54.615	3.07E+06	0.6	0.82

Average solute resistance to diffusion, K (s/m)	2.24E+06
Water permeability coefficient, A (m/atm·s)	3.13E-07
Mass transfer coefficient, k (m/s)	1.74E-05

7.1 Effect of mass transfer variation

Average solute resistance to diffusion, K (s/m)	2.24E+06
Water permeability coefficient, A (m/atm·s)	3.13E-07
Mass transfer coefficient, k (m/s)	1.74E-05

7.1.1 Seawater

Bulk draw solution osmotic pressure (atm)	Mass transfer coefficient variation	Feed solution mass transfer coefficient (m/s)	Predicted flux (L/m^2h)	$\pi_{F,m}$	$\pi_{F,m}/\pi_{F,b}$
	0.1k	1.74E-06	0.672	36.17	1.138979
54.62492	0.5k	8.70E-06	0.796	32.59	1.026368
Bulk feed solution osmotic pressure (atm)	k	1.74E-05	0.815	32.17	1.013098
	1.5k	2.61E-05	0.822	32.03	1.008713
31.75449	2k	3.48E-05	0.825	31.96	1.006528

7.1.2 Brackish water

Bulk draw solution osmotic pressure (atm)	Mass transfer coefficient variation	Feed solution mass transfer coefficient (m/s)	Predicted flux (L/m^2h)	$\pi_{F,m}$	$\pi_{F,m}/\pi_{F,b}$
	0.1k	1.74E-06	2.796	6.45	1.647564
54.62492	0.5k	8.70E-06	3.091	4.32	1.105016
Bulk feed solution osmotic pressure (atm)	k	1.74E-05	3.128	4.11	1.051197
	1.5k	2.61E-05	3.140	4.05	1.033847
3.913059	2k	3.48E-05	3.146	4.01	1.025279

8. Copper sulfate Flux

Feed solution concentration (ppm)	Feed solution osmotic pressure (atm)	Draw solution concentration (ppm)	Draw solution osmotic pressure (atm)	K (s/m)	Experimetnal flux (L/m^2h)	Predicted flux (L/m^2h)
5000	3.914	200000	26.64	1.35E+06	3.57	3.47

Average solute resistance to diffusion, K (s/m)	1.35E+06
Water permeability coefficient, A (m/atm·s)	3.13E-07
Mass transfer coefficient, k (m/s)	1.74E-05

8.1 Effect of mass transfer variation

Average solute resistance to diffusion, K (s/m)	1.35E+06
Water permeability coefficient, A (m/atm·s)	3.13E-07
Mass transfer coefficient, k (m/s)	1.74E-05

8.1.1 Brackish water

Bulk draw solution osmotic pressure (atm)	Mass transfer coefficient variation	Feed solution mass transfer coefficient (m/s)	Predicted flux (L/m^2h)	$\pi_{F,m}$	$\pi_{F,m}/\pi_{F,b}$
	0.1k	1.74E-06	3.061	7.01	1.791593
26.6463	0.5k	8.70E-06	3.584	4.40	1.123694
Bulk feed solution osmotic pressure (atm)	k	1.74E-05	3.653	4.15	1.060044
	1.5k	2.61E-05	3.675	4.07	1.039639
3.913059	2k	3.48E-05	3.687	4.03	1.029584

9. Effect of solute resistance to diffusion variation

Bulk draw solution osmotic pressure (atm)		K (s/m)	Predicted flux (L/m^2h)	$\pi_{D,i}$ (atm)	$\pi_{D,i}/\pi_{D,b}$
	0.1K	1.61E+05	6.454	53.18	0.973523
54.62492	0.5K	8.05E+05	2.040	47.77	0.874444
Feed solution osmotic pressure (atm)	K	1.61E+06	0.606	41.77	0.764653
	2K	3.22E+06	0.578	31.94	0.584694
31.75449	2.5K	4.03E+06	0.467	27.93	0.511282

Solute resistance to diffusion, K (s/m)	1.61E+06
Water permeability coefficient, A (m/atm·s)	3.13E-07
Mass transfer coefficient, k (m/s)	1.74E-05

10. Magnesium sulfate and copper sulfate flux comparison

	Draw solution osmotic pressure (atm)	Feed solution osmotic pressure (atm)	K (s/m)	Feed mass transfer coefficient (m/s)	Water permeability coefficient (m/atm·s)	Predicted flux (L/m^2h)
Copper sulfate	26.7	4	1.35E+06	1.74E-05	3.13E-07	3.46
Magnesium sulfate	26.7	4	2.24E+06	1.74E-05	3.13E-07	2.34

11. Effect of feed water concentration on membrane support to bulk osmotic pressure ratio- NaCl draw solution

Feed solution concentration (ppm)	Draw solution concentration (ppm)	Bulk draw solution osmotic pressure (atm)	$\pi_{D,i}$ (atm)	$\pi_{D,i}/\pi_{D,b}$
5030	80000	65.738941	13.4418	0.204474
10150	80000	65.738941	13.8567	0.210784
19500	80000	65.738941	18.6705	0.28401
31300	80000	65.738941	26.5468	0.403823
39000	80000	65.738941	32.3214	0.491663

Appendix B

Publications

R. Alnaizy, A. Aidan, M. Qasim, M. Almazrooei. “External and internal concentration polarization effects on Forward Osmosis permeate Flux”, editing for publication in *Journal of Environmental Chemical Engineering*, 2013.

References

[1] "About the Decade." Internet: http://www.un.org/waterforlifedecade/ background.shtml [May. 12, 2013].

[2] F. Rijsberman. (2005, Aug). "Water scarcity: Fact or fiction?" *Agricultural Water Management*.[online]. 80(1-3), pp.5-22. Available: http://www. sciencedirect.com. ezproxy.aus.edu/science/article/pii/S0378377405002854 [Dec. 26, 2012].

[3] "Statistica: Graphs & Maps." Internet: http://www.unwater.org/statistics_use.html. [Apr. 30, 2013].

[4] B. Freeman, B. Marrot, D. Lawler, L. Greenlee and P. Moulin. (2009, Mar.). "Reverse osmosis desalination: water sources, technology, and today's challenges." *Water Research*. [online]. 43(9), pp.2317-2348. . Available: http://www.sciencedirect. com. ezproxy.aus.edu/science/article/pii/ S0043135409001547. [Dec. 23, 2012].

[5] H. El-Dessouky, H. Ettouney, F. Al-Juwayhel and H. Al-Fulaij. (2004, Aug.)."Analysis of Multistage Flash Desalination Flashing Chambers." *Chemical Engineering Research and Design*. [online]. 82(8), pp.967-978. Available: http://www. sciencedirect. com.ezproxy.aus.edu/science/article/pii/ S0263876204725782 [Jul. 6, 2012]

[6] R. Mcllvaine. (2008, Aug.). "Reverse osmosis." *Chemical Engineering*.[online]. 115(8), pp.20-24.Available:http://search.proquest.com/docview/194446382? accountid=16946 [Dec. 13, 2012].

[7] M. Bourke. "Forward osmosis: a great leap forward for water treatment or a false start." Internet: http://michaelswatercooler.blogspot.ae/2010/09/forward-osmosis-great-leap-forward-for.html, Sep. 1, 2010 [Dec. 20, 2012].

[8] B. Buecker. *Power plant water chemistry: a practical guide*. Tulsa, OK: PennWell, 2006, pp.136-140.

[9] C. Boo, M. Elimelech, S. Hong and S. Lee. (2010, Dec)."Comparison of fouling behavior in forward osmosis (FO) and reverse osmosis (RO)."*Journal of Membrane Science*. [online]. 365 (1-2) pp.34-39. Available: http://www.sciencedirect.com. ezproxy.aus.edu/ science/article/pii/ S0376738810006666. [Nov. 13, 2012].

[10] N. A. Thompson and P. G. Nicoll. "Forward osmosis desalination: a commercial reality," presented at International Desalination Association World Congress, Perth, Australia, 2011.

[11] C. Tang, D. Mulcahy, L. Zou and S. Zhao. (2012, Apr.). "Recent developments in forward osmosis: opportunities and challenges." *Journal of Membrane Science*. [online]. 396, pp.1-21. Available: http:// www.sciencedirect.com.ezproxy.aus. edu/science/article/ pii/S0376738811009215 [Nov. 13, 2012].

[12] T.S. Chung, S. Zhang, K. Y. Wang, J. Su and M. M. Ling. (2012, Jan). "Forward osmosis processes: Yesterday, today and tomorrow." *Desalination.* [online]. 287, pp78-81. Available: http://www.sciencedirect.com.ezproxy.aus.edu/science/ article/pii/S0011916410009392 [Feb. 24, 2013].

[13] J. McCutcheon, R. McGinnis and M. Elimelech. (2006, Jan.). "Desalination by ammonia-carbon dioxide forward osmosis: influence of draw and feed solution on process performance." *Journal of Membrane Science*. [online]. 278, pp. 114-123. Available: http://www.sciencedirect.com.ezproxy.aus.edu/science/article/pii/ S0376738805007982 [Jan. 30, 2013].

[14] A. Childress, M. Elimelech and T. Cath. (2006, Jun.). "Forward osmosis: principles, applications, and recent developments." *Journal of Membrane Science*. [online]. 281(1-2), pp. 70-87. Available: http://www.sciencedirect.com.ezproxy.aus.edu/ science/article/pii/S0376738806003838 [Dec. 4, 2012].

[15] N. Hancock, R. McGinnis, and M. Nowosielski-Slepowron, G. McGurgan. (2013, Jan.). "Pilot demonstration of the NH3/CO2 forward osmosis desalination process on high salinity brines." *Desalination.* [online]. 312, pp.67-74. Available: http:// www.sciencedirect.com. ezproxy.aus.edu/science/article/pii/S0011916412006406 [Apr. 30, 2013].

[16] C. Suh and S. Lee. (2013, Jan). "Modeling reverse draw solute flux in forward osmosis with external concentration polarization in both sides of the draw and feed solution." *Journal of Membrane Science.* [online]. 427, pp. 365-374. Available: http://www.sciencedirect.com/science/article/pii/S0376738812006321 [Jul. 25, 2013].

[17] J. McCutcheon and M. Elimelech. (2006, Aug.). "Influence of concentrative and dilutive internal concentration polarization on flux behavior in forward osmosis." *Journal of Membrane Science.* [online]. 284(1-2), pp. 237-247. Available: http:// www. sciencedirect.com.ezproxy.aus.edu/ science/article/pii/S0376738806005 [Nov. 13, 2012].

[18] A. Achilli, T. Cath and A. Childress. (2010, Aug). "Selection of inorganic-base draw solutions for forward osmosis applications." *Journal of membrane science.* [online]. 364, pp. 233-241. Available: http://www.sciencedirect.com.ezproxy. aus.edu/science/article/pii/ S037673881000640X [Apr. 21, 2013].

[19] W. M. Haynes, CRC Handbook of Chemistry and Physics, 92d ed., National Institute of Standards and Technology, Boulder, CO, 2011.

[20] I. L. Alsvik and M. B. Hagg. (2013, Mar). "Pressure retarded osmosis and forward osmosis membrane materials and methods." *Polymers.* [online]. 5, pp. 303-327. Available: http://www.mdpi.com/2073-4360/5/1/303. [Apr. 14, 2013].

[21] M. Sairam, E. Sereewatthanawut, K. Li and A. Livingston. (2011, Feb). "Method for the preparation of cellulose acetate flat sheet composite membranes for forward osmosis-desalination using MgSO4 draw solution." *Desalination*. [online]. 273, pp.299-307. Available: http://www.sciencedirect.com.ezproxy.aus.edu/science/article/pii/S0011916411000610 [Apr. 17, 2013].

[22] J. Su, Q. Yang, J. Teo and T. Chung. (2010, Mar.). "Cellulose acetate nanofiltration hollow fiber membranes for forward osmosis processes." *Journal of membrane science.* [online]. 355, pp.36-44. Available: http://www.sciencedirect.com.ezproxy.aus.edu/science/article/pii/S0376738810002115 [Apr. 17, 2013].

[23] R. Ong, T. Chung, B. Helmer and J. Wit. (2012, Nov.). "Novel cellulose ester for forward osmosis membranes." *Industrial & engineering chemistry research*. [online]. 51, pp.16136-16145. Available: http://www3.aiche.org/Proceedings/Abstract. aspx?PaperID=275657 [Apr. 16, 2013].

[24] S. Loeb, L. Titelman, E. Korngol and J. Freeman. (1997, Jan). "Effect of porous support fabric on osmosis through a Loeb-Sourirajan type asymmetric membrane." *Journal of membrane science.* [online]. 129, pp. 243-249. Available: http://www.sciencedirect.com.ezproxy. aus.edu/science/article/pii/S0376738896003547 [Mar. 27, 2013].

[25] J. McCutcheon and M. Elimelech. (2007, Jul). "Modeling water flux in forward osmosis: implications for improved membrane design."*AIChE Journal*. [online]. 53(7), pp. 1736-1744. Available: www.interscience.wiley.com [Sep.1, 2012].

[26] A. Yokozeki. (2006, Jan.). "Osmotic pressures studied using a simple equation-of-state and its applications." *Applied Energy*. 83 (1), pp. 15-41. http://ac.els-cdn.com.ezproxy.aus.edu/ S0306261904002016/1-s2.0-S0306261904002016-main.pdf?_tid=d04e4268-cd34-11e2-86f3-00000aab0f6b&acdnat=1370363929_5e4970f1a38b1d89f019981fce2c2107 [Jun 4, 2013].

[27] HYSYS OLI interface: reference guide. Aspen Technology Inc., Cambridge, MA, 2003. [online]. Internet: http://www.ece.jcu.edu.au/ subjects/cl4070/HySyS%20documentation/Doc/HYSYS/OLI.pdf [Jun. 16, 2013].

[28] J. Hoffman. *Numerical methods for engineers and scientists.* Boca Raton, FL: CRC press, 2001, pp.146.

[29] G. Gray, J. McCutcheon, and M. Elimelech. (2006, Feb.). "Internal concentration polarization in forward osmosis: role of membrane orientation." *Desalination*. [online]. 197(1-3), pp.1-8. Available: http://www.sciencedirect.com.ezproxy.aus.edu/science/article/pii/ S0011916406010605 [Nov. 17, 2012].

[30] C.H. Tan and H.Y. Ng. (2008, Jul.). "Modified models to predict flux behavior in forward osmosis in consideration of external and internal concentration polarization." *Journal of Membrane Science.* [online]. 324, pp.209-219. Available: http://www.sciencedirect. com.ezproxy.aus.edu/science/article/pii/ S0376738808006741[Jun. 8, 2013].

Vita

Muna Al Mazrooei was born in Dubai. She graduated from Dubai National School and joined the American University of Sharjah in 2005. She graduated in 2009 with a Bachelor of Science degree in Chemical Engineering.

She started working at Dubai Aluminum ‘Dubal’ in February 2010 as Power and Desalination Chemist and joined the Master’s degree program in February 2011.